Aus dem Institut für Neuropathologie
der Medizinischen Fakultät Charité – Universitätsmedizin Berlin

DISSERTATION

Autophagy in Microglia and Alzheimer's disease

zur Erlangung des akademischen Grades
Doctor of Philosophy (PhD)

vorgelegt der Medizinischen Fakultät
Charité – Universitätsmedizin Berlin

von

Judith Houtman

aus Gouda, die Niederlande

Datum der Promotion: 06.09.2019

Index

Abstract

Alzheimer's disease (AD) is the most common neurodegenerative disease, characterized by amyloid-beta plaques, neurofibrillary tangles and neuroinflammation. Autophagy has been associated with several neurodegenerative diseases. Recently, autophagy has been linked to the regulation of the inflammatory response in macrophages. My thesis investigates how an impairment of autophagy influences the inflammatory response of microglia. We used Beclin1 heterozygous (*Becn1*$^{+/-}$) mice as a model of impaired autophagy. Beclin1 plays a role in the initiation of autophagy and was shown to be decreased in microglia isolated from AD patients compared to healthy controls. *In vitro*, acutely stimulated microglia from neonatal *Becn1*$^{+/-}$ mice exhibited increased expression of the proinflammatory cytokines IL-1beta and IL-18 compared to wild type microglia. Both IL-1beta and IL-18 are processed by the NLRP3 inflammasome pathway. The investigation of this pathway showed an elevated number of cells with inflammasomes and increased levels of the inflammasome components NLRP3 and cleaved Caspase1 in *Becn1*$^{+/-}$ microglia. Super resolution microscopy revealed a very close association of NLRP3 aggregates and LC3-positive autophagosomes. Interestingly, despite suggestions that the murine CALCOCO2 does not function as an autophagic adaptor, we discovered CALCOCO2 colocalised with NLRP3 and that its downregulation by siRNA knockdown increased IL-1beta release. These data support the notion that selective autophagy can impact microglia activation by modulating IL-1beta and IL-18 production via NLRP3 degradation. These *in vitro* data present a mechanism how impaired autophagy could contribute to neuroinflammation in AD.
In vivo analysis of *Becn1*$^{+/-}$*.APPPS1* mice also demonstrated enhanced IL-1beta levels, but no differences in amyloid beta pathology, nor phagocytic capacity. The constitutive heterozygosity of Beclin1 might be responsible for the milder effects *in vivo*. Therefore, we performed studies utilizing more sophisticated models targeting immune cells specifically. The first model, *Aldh1l1-iCre.Becn1-flox*, targets *Becn1* deletion specifically in astrocytes in the central nervous system after injection with the drug tamoxifen. Peripherally, Aldh1l1 is also expressed by hepatocytes. The *Aldh1l1-iCre.Becn1-flox* mice suffered from peripheral damage in the liver 10 days after tamoxifen injection, and can therefore not be used in further studies. The second model, *Cx3Cr1-iCre.Becn1-flox*, targets *Becn1* deletion specifically in microglia in the central nervous system, and will be crossed to the *APPPS1* mice to create a tool to study the role of Beclin1 in microglia in neuroinflammation and neurodegeneration. This new tool and the data generated in this work will support a new direction of research, to unravel the therapeutic potential of autophagy-dependent inflammation in neurodegenerative diseases.

Zusammenfassung

Die Alzheimer-Krankheit (AD) ist die häufigste neurodegenerative Erkrankung, die durch Amyloid-Beta-Plaques, neurofibrilläre Verwicklungen und Neuroinflammation gekennzeichnet ist. Autophagie wurde mit mehreren neurodegenerativen Erkrankungen in Verbindung gebracht. Vor Kurzem wurde Autophagie mit der Regulierung der Entzündungsreaktion in Makrophagen in Verbindung gebracht. Meine Dissertation untersucht, wie eine Beeinträchtigung der Autophagie die Entzündungsreaktion von Mikroglia beeinflusst. Wir haben Beclin1-heterozygote (*Becn1*$^{+/-}$) Mäuse als Modell für eingeschränkte Autophagie verwendet. Beclin1 spielt eine Rolle bei der Initiierung der Autophagie und es wurde gezeigt, dass es bei aus AD-Patienten isolierten Mikrogliazellen im Vergleich zu gesunden Kontrollen abnimmt. Akut stimulierte Mikroglia aus neonatalen *Becn1*$^{+/-}$ Mäusen zeigten *in vitro* eine erhöhte Expression der proinflammatorischen Zytokine IL-1beta und IL-18 im Vergleich zu Wildtyp-Mikroglia. Sowohl IL-1beta als auch IL-18 werden vom NLRP3-Inflammasom-Weg verarbeitet. Die Untersuchung dieses Weges zeigte eine erhöhte Anzahl von Zellen mit Inflammasomen und erhöhte Spiegel der Inflammasomenkomponenten NLRP3 und gespaltenen Caspase1 in *Becn1*$^{+/-}$ Mikroglia. Super-Resolution-Mikroskopie zeigte eine sehr enge Lokalisation von NLRP3-Aggregaten und LC3-positiven Autophagosomen. Interessanterweise haben wir trotz der Kritik, dass das murine CALCOCO2 nicht als autophagischer Adapter fungiert, entdeckt, dass CALCOCO2 mit NLRP3 kolokalisiert und dass die Herunterregulierung durch siRNA die IL-1beta-Freisetzung erhöhte. Diese Daten stützen die Ansicht, dass selektive Autophagie die Mikroglia-Aktivierung beeinflussen kann, indem die IL-1beta- und IL-18-Produktion durch NLRP3-Abbau moduliert wird. Diese *in vitro* Daten stellen einen Mechanismus dar, wie eine gestörte Autophagie zur Neuroinflammation bei AD beitragen kann.
In vivo Analysen von *Becn1*$^{+/-}$*.APPPS1* Mäusen zeigten ebenfalls erhöhte IL-1beta-Spiegel, jedoch keine Unterschiede in der Amyloid-Beta-Pathologie und auch keine in Bezug auf die Phagozytosekapazität. Die konstitutive Heterozygotie von Beclin1 könnte für die geringen Auswirkungen *in vivo* verantwortlich sein. Daher etablierten zwei neue Modelle, die speziell auf Immunzellen abzielten. Das erste Modell, *Aldh1l1-iCre.Becn1-Flox*, zielt auf die Becn1-Deletion spezifisch in Astrozyten im zentralen Nervensystem nach Injektion des Arzneimittels Tamoxifen ab. In der Peripherie wird Aldh1l1 auch von Hepatozyten exprimiert. Die *Aldh1l1-iCre.Becn1-Flox* Mäuse erlitten 10 Tage nach Tamoxifen-Injektion eine periphere Schädigung der Leber und können daher nicht in weiteren Studien verwendet werden. Das zweite Modell, *Cx3Cr1-iCre.Becn1-flox*, zielt auf die Becn1-Deletion speziell in Mikroglia im Zentralnervensystem ab und wird mit den *APPPS1*-Mäusen gekreuzt, um ein Modell für die Untersuchung der Rolle von Beclin1 in Mikroglia bei Neuroinflammation und Neurodegeneration darzustellen. Dieses neue Mausmodell und die in dieser Arbeit generierten Daten werden eine neue Richtung der Forschung unterstützen, um das therapeutische Potenzial autophagieabhängiger Entzündungen bei neurodegenerativen Erkrankungen zu ermitteln.

The role of Beclin1 in neuroinflammation and Alzheimer's disease

BACKGROUND

Alzheimer's disease

Alzheimer's disease (AD) is the most common neurodegenerative disease, with increasing prevalence in our aging society (Querfurth & LaFerla, 2010). The disease was first described by Alois Alzheimer in the beginning of the 1900s who found extracellular protein aggregates and intraneuronal fibers in patient tissue. The co-existence of extracellular amyloid-beta (Abeta) plaques and intracellular phosphorylated tau tangles are still considered as the hallmarks of AD pathology and are routinely used for diagnosis (Montine, Phelps et al, 2012). Despite uncovering parts of the disease-related mechanisms, a treatment or a cure for this devastating disease is still far from being found.

One of the more recent discoveries in the field of AD research is the influence of glial cells and neuroinflammation upon pathophysiology. The importance of non-neuronal cells in maintaining brain homeostasis and responding to danger signals has long been neglected but is now becoming increasingly relevant. The exact role of neuroinflammation in the pathology of AD remains debated. It was assumed that the plaques and tangles activate the brain's intrinsic immune cells, namely microglia and astrocytes, inducing the release of pro-inflammatory cytokines and chemokines. In line with this hypothesis, microgliosis and astrogliosis as well as complement-activated oligodendrocytes can all be found in the cortex and hippocampus, the brain regions affected by AD pathology. However, wild type mice challenged prenatally with the viral mimic PolyI:C develop an AD-like phenotype (Krstic, Madhusudan et al, 2012), leading to a new hypothesis that neuroinflammation might occur much earlier in the disease, and can be considered a driver of pathology rather than a consequence (Heppner, Ransohoff et al, 2015). This hypothesis opened up a new possible treatment approach through targeting the AD pathophysiology via immunomodulation.

Immunomodulation is based on the idea that microglia, the innate immune cells of the brain, are able to phagocytose Abeta, therefore counteracting the aggregation of Abeta into pathological plaques. Upon uptake of Abeta, the mechanisms of its degradation are still unclear. One potential pathway of removing intracellular Abeta is via macro-autophagy (referred to as autophagy).

Autophagy

Autophagy has been associated with several neurodegenerative diseases and aging. This well-preserved pathway is present in organisms ranging from yeast to human, and found in every cell of the human body. The main purposes of autophagy are to maintain cell homeostasis and to prevent cell death by degrading large proteins or protein aggregates that cannot be targeted by the proteasome due to their size. Such large proteins are removed in an organized manner via the formation of autophagosomes (Fig. 1). Here, protein complexes

of several autophagy-related proteins (ATGs) create a double membrane. Autophagic adaptor proteins connect to the cargo and transfer the cargo to the double membrane of the phagophore. Once the cargo attaches to the membrane it closes and the autophagosome fuses with a lysosome to allow for degradation of the cargo into amino acids by proteases in an acidic environment. Finally, the autolysosome is broken down which releases the amino acids to be re-used as building blocks for new proteins (see Fig. 1, reviewed in more detail in (Menzies, Fleming et al, 2015)).

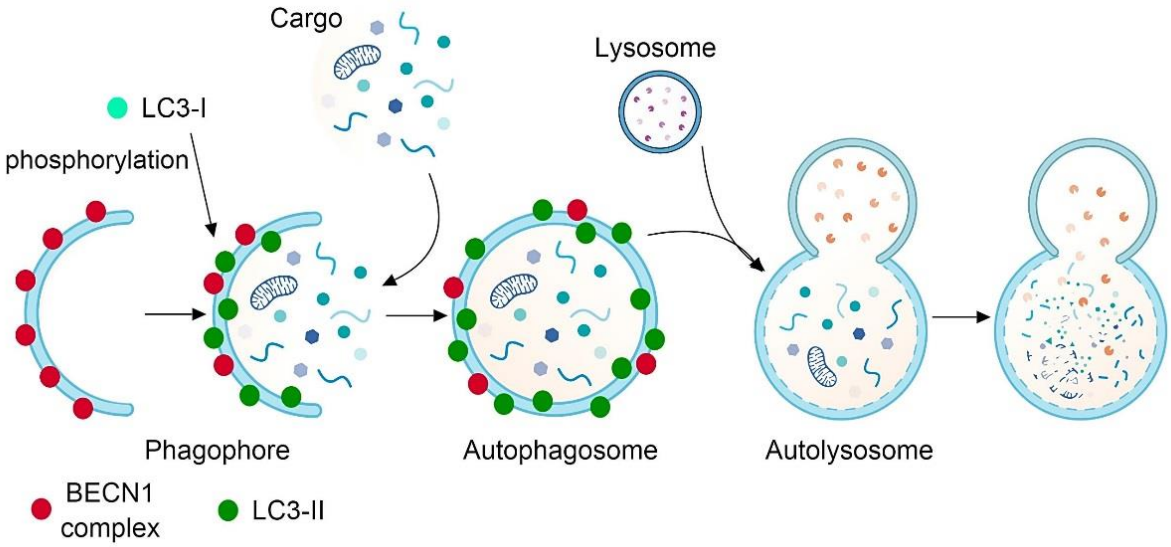

Figure 1. Schematic representation of the autophagy pathway

Protein complexes, like the BECN1 complex, initiate vesicle nucleation by forming a double membrane, called the phagophore. LC3-I is phosphorylated upon the formation of the phagophore, and recruited to the membrane as LC3-II. A cytoplasmic cargo is bound by autophagic adaptor proteins and shuttled towards the phagophore. Once the adaptor protein carrying the cargo binds to LC3-II on the phagophore, the membrane closes and forms an autophagosome. The autophagosome fuses with a lysosome to an autolysosome. The content of the autolysosome is degraded by the proteases in acidic pH. The degraded content is released back into the cytoplasm to be re-used by the cell. (designed with Biorender, based on (Yang, Kaushal et al, 2008))

During the aging process autophagy becomes impaired, leading to the hypothesis that decreased autophagy is one of the causes of age-induced neurodegenerative diseases (Menzies, Fleming et al, 2015). In support of this hypothesis, Pickford *et al*. could show that autophagy levels negatively correlate with neurodegenerative disease by comparing Beclin1 (BECN1/ATG6) levels in cortex samples of AD patients, patients with mild cognitive impairment and healthy age-matched controls (Pickford, Masliah et al, 2008). BECN1 is a multifunctional protein with roles in: autophagy, inducing vesicle nucleation (Suzuki, Kubota et al, 2007); phagocytosis, by recycling transmembrane receptors (Lucin, O'Brien et al, 2013); neuroprotection, by controlling TGF-beta signaling (O'Brien, Bonanno et al, 2015); and development, illustrated by the embryonic lethality of *Becn1*$^{-/-}$ mice (Yue, Jin et al, 2003). The *Becn1*$^{+/-}$ mouse is used as an alternative model and does not show an abnormal phenotype, apart from a higher incidence of tumors at a later age (Qu, Yu et al, 2003).

Pickford *et al*. crossed the *Becn1*$^{+/-}$ mice to AD-like T41 mice, and showed that a decreased level of autophagy in these mice led to a worsening of Abeta pathology (Pickford, Masliah et al, 2008).

Maintaining cell homeostasis is especially important for long-lived cells, such as neurons, and the decrease in BECN1 in the human cortex samples was therefore mainly attributed to neuronal autophagy levels. However, a significant decrease in BECN1 protein levels was found in microglia isolated from AD patients several years later (Lucin, O'Brien et al, 2013). This postulated a correlation between the immune system and autophagy, which could have downstream effects upon neurodegenerative processes.

Autophagy in innate immunity

Several studies have investigated the role of autophagy in inflammation, depleting different tissue macrophages of the autophagic proteins ATG5 (Lodder, Denaës et al, 2015), ATG7 (Lee, Kim et al, 2016) or ATG16L1 (Saitoh, Fujita et al, 2008). The lack of these proteins worsened inflammatory diseases in different models (Lee, Kim et al, 2016; Lodder, Denaës et al, 2015; Saitoh, Fujita et al, 2008), or induced pro-inflammatory cytokine release *in vitro* (Ye, Jiang et al, 2017). This data supports the hypothesis that decreased autophagy in peripheral macrophages correlates with an exacerbation of immunological diseases.

Within the central nervous system, microglia are the first line of defense, and were therefore previously addressed as brain macrophages. However, recently it was discovered that microglia derive from the yolk sac at E9.5, rather than from hematopoietic cells like other tissue macrophages (Ginhoux, Greter et al, 2010). This difference in ontogeny is also shown in their genetic signature, making microglia a special group of phagocytic immune cells (Hickman, Kingery et al, 2013). Recent discoveries support that the combination of ontogeny and the CNS environment accounts for a unique microglial identity (Bennett, Bennett et al, 2018). Thus, we should be careful transferring our knowledge of macrophages directly to microglia. Regarding autophagy, only few studies focused specifically on microglia, with conflicting results. François *et al.* studied LPS treated microglia and showed no relation between cytokine release and blockage of autophagy (François, Terro et al, 2013). In another study, Cho *et al*. investigated the role of Abeta and autophagy in microglia, showing that fibrillary Abeta is degraded by autophagy, and that fibrillary Abeta-induced NLRP3 inflammasome activation is increased in *Atg5*$^{-/-}$ microglia (Cho, Cho et al, 2014).

AIM

Since the literature describes a role for autophagy in inflammation and linking decreased BECN1 protein levels to neurodegeneration, we hypothesized that microglial BECN1 plays a role in neuroinflammation, and set out to discover which pathways are involved.

RESULTS AND DISCUSSION

Becn1 heterozygosity in vitro

As a first step, we analyzed the BECN1 levels in *Becn1*$^{+/-}$ and wild type neonatal microglia, which showed a ~40% reduction of BECN1 in *Becn1*$^{+/-}$ microglia (Houtman, Freitag et al, 2019). Next, the inflammatory response of *Becn1*$^{+/-}$ and wild type neonatal microglia was analyzed *in vitro*. Wild type as well as *Becn1*$^{+/-}$ microglia were treated with the commonly used inflammatory stimuli combination of LPS and ATP. The binding of LPS to TLR4 led to the release of pro-inflammatory cytokines like TNF-alpha and IL-6 (interleukin 6), and subsequent exposure to ATP released IL-1beta and IL-18 (Houtman, Freitag et al, 2019). Interestingly, the *Becn1*$^{+/-}$ microglia, showing a decreased amount of autophagy, released more IL-1beta and IL-18 than wild type microglia. Both of these cytokines are cleaved to gain their activated form by the NLRP3 inflammasome (Fig. 2).

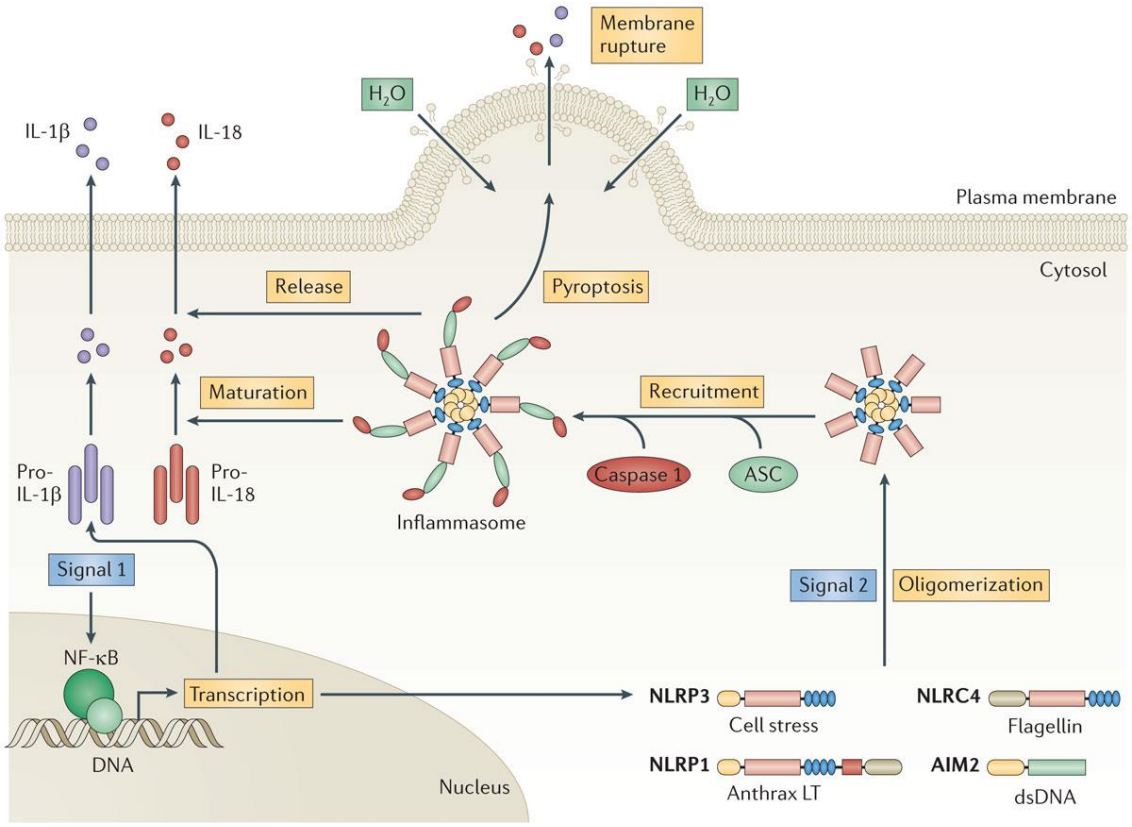

Figure 2. Schematic representation of the inflammasome pathway (Walsh, Muruve et al, 2014)
Binding of the TLR4 receptor by signal 1, for instance LPS, primes the inflammasome pathway. Pro-IL-1beta and pro-IL-18 are transcribed and translated, as well as NLRP3. A second signal, for instance ATP, causes the NLRP3 molecules to oligomerize and recruit ASC and Caspase 1. This protein complex called the inflammasome releases the activated form of Caspase 1, cleaves pro-IL-1beta and pro-IL-18, upon which the active forms of the cytokines are released.

As presented in our publication (Houtman, Freitag et al, 2019), we discovered that several components of the NLRP3 inflammasome – NLRP3 protein level, ASC specks and activated caspase 1 – are increased in *Becn1*$^{+/-}$ microglia. Immunocytochemistry of *Becn1*$^{+/-}$ microglia showed colocalization of NLRP3 with LC3, a protein found on the autophagosomal

membrane. Super resolution microscopy (Structured Illumination Microscopy, SIM) and subsequent radial plot analysis confirmed that NLRP3 and LC3-II were located on the same organelle, supporting the link of autophagy to inflammation (Houtman, Freitag et al, 2019).

After defining the relevance of BECN1 in autophagy in the response to inflammatory stimuli, we aimed at uncovering other pathways that could be affected by BECN1 in an inflammatory setting.

Phagocytosis

As BECN1 is known to play a role in retromer recycling of transmembrane receptors involved in phagocytosis (Lucin, O'Brien et al, 2013), we investigated the phagocytic capacity of *Becn1*$^{+/-}$ microglia. As described in Houtman et al., we performed an *ex vivo* slice assay based on an earlier publication from our lab (Krabbe, Halle et al, 2013). Comparing *Becn1*$^{+/-}$ and wild type animals of 4 months old, we did not observe any difference in phagocytic capacity (Houtman, Freitag et al, 2019).

In order to check the phagocytic capacity of neonatal microglia, we established the pHrodo *E. coli* bioparticles assay (see methods section below). When comparing neonatal wild type microglia with neonatal *Becn1*$^{+/-}$ microglia we did not observe any difference in phagocytic capacity (Fig 3A).

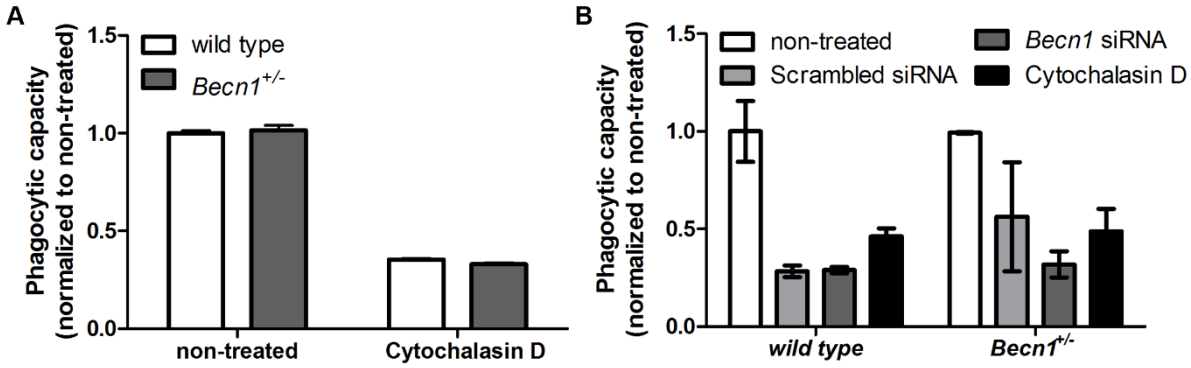

Figure 3. Phagocytosis assays with neonatal microglia

A) The pHrodo bead assay is able to measure phagocytosis of neonatal wild type and *Becn1*$^{+/-}$ microglia. Cytochalasin D is a pharmaceutical impairing actin filament polymerisation, which also blocks phagocytosis, and is used as a negative control. Phagocytic capacity was normalized to wild type non-treated samples. There is no difference in phagocytic capacity between wild type and *Becn1*$^{+/-}$ microglia. N = 3. B) The pH rodo bead assay performed on siRNA treated neonatal microglia. The siRNA treatment itself (scrambled siRNA control) blocked phagocytic capacity in a similar manner as cytochalasin D. N=3.

Since BECN1 protein levels in *Becn1*$^{+/-}$ microglia are only reduced by 50%, the remaining protein could still influence phagocytosis. We therefore performed an siRNA knockdown of *Becn1* in the *Becn1*$^{+/-}$ microglia to achieve a stronger reduction of BECN1 protein expression. Unfortunately, the siRNA treatment itself affected phagocytic capacity, since the scrambled siRNA treated cells presented with decreased phagocytic capacity as well (Fig 3B). Thus, in

our hands the partially depleted BECN1 levels did not influence phagocytic capacity, which is contrary to previously published results (Lucin, O'Brien et al, 2013). This discrepancy could be due to different experimental approaches. Lucin *et al*., utilized BV2 cells with a strong BECN1 knockdown, an immortalized microglia cell line that is genetically very different from microglia (Das, Kim et al, 2016), for their phagocytosis experiments. Additionally, Lucin *et al.* employed different assays to assess phagocytic capacity.

Based on the increase of the inflammasome components in the *Becn1*$^{+/-}$ microglia, the colocalization of NLRP3 and LC3 as well as the lack of change in phagocytic capacity in the *Becn1*$^{+/-}$ cells, we specified our hypothesis from 'microglial BECN1 plays a role in neuroinflammation' to 'microglial autophagy regulates neuroinflammation by degrading NLRP3'.

CALCOCO2 as possible autophagic adaptor

In support of this hypothesis, we discovered a relation between CALCOCO2/NDP52 and NLRP3 as well as between CALCOCO2 and IL-1beta release (Houtman, Freitag et al, 2019). CALCOCO2 is described as one of the autophagic adaptor proteins, responsible for shuttling cargo to the autophagosomal membrane.

Within the community, there are some doubts that CALCOCO2 exists and is functional in mice. In order to proof that it exists and functions, we performed an extensive literature study and found NCBI records of the validated mRNA (NM_001271018.1) and amino acid (NP_001257947.1) sequences of murine Calcoco2 in the NCBI gene and protein bank. On top of that, a comparison between the protein sequence of human (isoform1) and murine NDP52 show 128 identical amino acids in the N-terminal region. This indicates that the murine NDP52 protein sequence as presented by Tumbarello *et al.* (Tumbarello, Manna et al, 2015) is related to the human one. Finally, using cDNA of murine microglia, the amplification of the coding sequence of murine CALCOCO2 resulted in a band of around 1000 bp. In western blots (with an antibody raised against the N-terminal domain of human NDP52/CALCOCO2) a band of about 34 kDa was detected (Fig. 5E of (Houtman, Freitag et al, 2019)), which is in agreement with the published coding sequence. Kim *et al.* also showed that murine NDP52 mRNA and protein has been detected in the brain of AD model mice (Kim, Lee et al, 2014).

Although we established the presence of CALCOCO2 in mice, we are also aware that the murine CALCOCO2 is truncated. On the other hand, the NCBI protein bank showed four additional alternatively spliced transcript variants of NDP52 that are all shorter, indicating possible functions of truncated NDP52 also in human cells.

The proteins can be dissected into domains, hNDP52 consists of a C-terminal LIM-like domain (zinc fingers), a Galectin-8 domain, an intermediate coiled coil domain, a non-canonical LC3-interacting region motif for LC3C interaction (LIR), and an N-terminal SKICH

domain. The truncated mNDP52 still contains the intermediate coiled coil domain, a non-canonical LC3-interacting region motif for LC3C interaction (LIR), and a N-terminal SKICH domain (see Fig. 4 as well as (Tumbarello, Manna et al, 2015)).

The domains that remain in murine CALCOCO2 have been shown to bind a number of proteins, and have been related to autophagy. The non-canonical LIR motif selectively binds LC3C, which recruits all ATG8 orthologues to the autophagosome (von Muhlinen, Akutsu et al, 2012). The SKICH domain of hNDP52 has been shown to bind phosphorylated tau and amyloid-beta (Jo, Gundemir et al, 2014), damaged mitochondria (Furuya, Kakuta et al, 2018), TRIF and TRAF6 (Inomata & Into, 2012). In the protein TAX1BP1/CALCOCO3 the SKICH domain is thought to be required for the autophagy function (Yang, Wang et al, 2015). The LIM-like domain that is missing in murine CALCOCO2 is responsible for ubiquitin binding, but autophagic degradation of for instance tau and amyloid-beta is suggested to be ubiquitin independent (Jo, Gundemir et al, 2014).

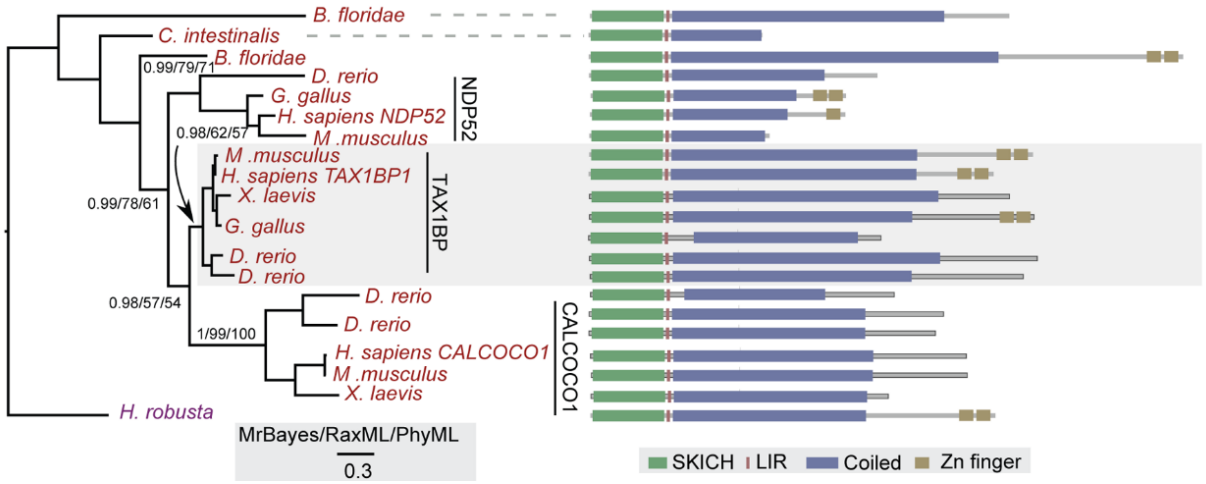

Figure 4. Evolutionary analysis of CALCOCO1, CALCOCO2/NDP52 and TAX1BP1/CALCOCO3
The analysis shows that murine CALCOCO2 has a truncated version of CALCOCO2, lacking the zinc finger domain. It also shows murine CALCOCO2 is related to the human variant. (Figure from (Tumbarello, Manna et al, 2015))

As presented in Houtman et al., immunocytochemistry showed a colocalization of NLRP3 and CALCOCO2 and further analysis by SIM confirmed this. A radial plot analysis of the SIM pictures showed that CALCOCO2 is significantly closer to NLRP3 than LC3, although NLRP3 and LC3 are still part of the same organelle. We used siRNA knockdown of CALCOCO2 in wild type neonatal microglia to confirm its relevance in the inflammasome pathway and indeed observed an increased release of IL-1beta (Houtman, Freitag et al, 2019).

We also performed an immunoprecipitation of NLRP3 with CALCOCO2, however, we did not obtain a convincing band. As autophagy is an ongoing process, the connection between NLRP3 and CALCOCO2 is only temporary. The lack of a band appears therefore to be rather a

technical limitation. The small percentage of cells displaying a colocalization of NLRP3 and CALCOCO2 in immunocytochemistry supports this hypothesis.

Based on the literature and the above mentioned data we conclude that, although the mouse NDP52 is truncated and therefore missing the ubiquitin-binding zinc finger domains, this does not mean it is dysfunctional per se. mNDP52 could still play a role in autophagy, most likely in a slightly different way as the traditional autophagy adaptors, since mNDP52 cannot bind ubiquitin. mNDP52 might require a second protein or a protein complex to connect the cargo to the phagophore. Future studies will have to unravel the exact mechanism. However, the domains that are present in mNDP52 have been shown to be relevant in autophagic degradation of different cargo types.

We propose that the role of mNDP52/CALCOCO2 in decreasing IL-1beta release is mediated via autophagy. We hypothesize autophagic degradation of the inflammasome by binding of NLRP3 to the SKICH domain and subsequent binding of LC3-II on the phagophore by the LIR domain present in mNDP52 or in complex with one or more additional proteins.

Taken together, our data show that the activity of the NLRP3 inflammasome is controlled by autophagy in microglia *in vitro*, and suggest CALCOCO2 might shuttle NLRP3 to the autophagosome. When autophagy is decreased like in *Becn1*$^{+/-}$ microglia, or levels of CALCOCO2 are decreased by siRNA knockdown, it leads to increased IL-1beta release.

Becn1 heterozygosity in vivo

The fascinating *in vitro* data prompted us to investigate *Becn1* heterozygosity *in vivo*. Until now, there was only one study analyzing *Becn1* heterozygosity and AD *in vivo*. Pickford *et al*. crossed *Becn1*$^{+/-}$ mice to the T41 AD-like mouse model, which reduced neuronal autophagy, disrupted lysosomes, promoted intracellular and extracellular Abeta accumulation, and resulted in neurodegeneration (Pickford, Masliah et al, 2008). We therefore investigated the link between autophagy-controlled inflammation and Abeta pathology by crossing *Becn1*$^{+/-}$ mice to another AD-like mouse model, *APPPS1* (Radde, Bolmont et al, 2006). *APPPS1* mice are characterized by a fast disease progression, showing their first plaques already at 2 months compared to 3-4 months in the T41 mice (Rockenstein, Mallory et al, 2001). We analyzed whole brain lysates of double transgenic *APPPS1.Becn1*$^{+/-}$ mice, single transgenic *APPPS1* and *Becn1*$^{+/-}$ mice, and wild type mice over time. When assessing pro-inflammatory cytokines, there was a significant increase in IL-1beta release in *APPPS1.Becn1*$^{+/-}$ mice compared to wild type mice at the age of 4- and 8-months. The brain lysates of *APPPS1* mice appeared to contain more IL-1beta, although this was not significant (Houtman, Freitag et al, 2019). Thus, the inflammasome pathway seems to be activated in response to Abeta pathology, yet a decrease in autophagy leads to significantly increased cytokine release. Despite these changes in the inflammatory milieu, Abeta load was unchanged between the *APPPS1* and *APPPS1.Becn1*$^{+/-}$ mice (Houtman, Freitag et al, 2019). Considering that we did not find a decrease in phagocytic capacity of *Becn1*$^{+/-}$ microglia, Abeta clearance is probably

also not affected in the *APPPS1* context, explaining why no effect upon amyloid beta pathology was seen. As mentioned before, *APPPS1* mice have a more aggressive pathology than T41 mice, as well as a presenilin mutation, which could explain why Pickford *et al.* did find a difference in Abeta pathology.
Since the model used is a constitutive *Becn1*$^{+/-}$ mouse, all cell types express only one *Becn1* allele. This might also play an additional role in the increased IL-1beta levels in this *in vivo* model. IL-1beta binds to the IL1 receptor that is ubiquitously expressed and activates many different pathways (Weber, Wasiliew et al, 2010). It is possible that the decreased BECN1 levels in the other CNS cells influence the uptake and degradation of IL-1beta, leading to increased IL-1beta levels.

Since the *in vitro* data did show a clear role for BECN1 and autophagy in controlling microglial inflammasome activity and IL-1beta and IL-18 release, we set out to create a more sophisticated model to link AD-pathology to autophagy and inflammation specifically via microglia.

Microglia-specific knockdown of Becn1
In order to generate a microglia specific and complete knockdown of *Becn1*, we decided to use an inducible Cre-flox system in *APPPS1* mice. First, *Cx3Cr1*^{CreERT} mice were crossbred to *Becn1*$^{flox/flox}$ mice. By putting the expression of the Cre recombinase under the control of the Cx3Cr1 promotor, gene excision is carried out specifically in microglia, intestinal macrophages and kidney macrophages, but not other myeloid cells (Yona, Kim et al, 2013). However, due to the higher proliferation rate of peripheral monocytes and macrophages, the gene deletion is microglia specific after approximately 7 weeks (Yona, Kim et al, 2013). In this model, Cre recombinase activation is also linked to estrogen receptor thymidine induction, which can be achieved by treatment with its agonist tamoxifen. In *Becn1*$^{flox/flox}$ mice, exons 4-7 of the *Becn1* gene are flanked by loxP sites, which are targeted by Cre recombinase and deleted via homologous recombination. When treating the *Cx3Cr1*^{CreERT}*.Becn1*$^{flox/flox}$ mice with tamoxifen, we can therefore induce deletion of *Becn1* specifically in microglia at any chosen time point.

To test the functionality of the *Becn1*$^{flox/flox}$ mice, we crossed them to *CMV*^{Cre} mice, constitutively expressing the Cre recombinase and therefore leading to an immediate knockout of exons 4-7 of *Becn1* throughout all cell types. Since a full *Becn1* knockout is embryonic lethal, we compared *CMV*^{Cre}*.Becn1*$^{wt/flox}$ to *CMV*^{wt}*.Becn1*$^{wt/flox}$ for the flox-excised gene by genotyping. Indeed, in *CMV*^{Cre}*Becn1*$^{wt/flox}$ mice a wild type and floxed-gene were detected via PCR whilst in *CMV*^{wt}*.Becn1*$^{wt/flox}$ only a wild type gene was amplified, confirming the functionality of the *Becn1*$^{flox/flox}$ mice (Fig. 5A).

To test the microglial-specific *Becn1* deletion in the *Cx3Cr1*^{CreERT}*.Becn1*$^{flox/flox}$ mice, we injected 60-day-old animals intraperitoneal with 75mg/kg tamoxifen diluted in olive oil, and a control group with just olive oil, for 5 consecutive days. Twenty days later, we sacrificed

the mice and isolated peritoneal macrophages, splenocytes, intestinal macrophages and microglia (see methods).
We could not confirm a tamoxifen-dependent deletion of microglial *Becn1* by genotyping (Fig. 5B). Further analysis of the mice revealed that the *Cx3Cr1*^{CreERT} mice still possessed the neomycin cassette. This cassette is used in the generation of transgenic mouse lines, and ought to be removed before use since it was shown to inhibit the expression level of the Cre recombinase (Kaartinen & Nagy, 2001). We therefore had to cross the *Cx3Cr1*^{CreERT} mice to the *CMV*^{Cre} mice to knockout the neomycin cassette, and then use the resulting strain to generate a functional *Cx3Cr1*^{CreERT}*.Becn1*$^{flox/flox}$ line.

To further test our hypothesis that 'microglial Beclin1 influences neuroinflammation via autophagy' *in vivo*, future research that is not part of this thesis, will start with characterizing the *Cx3cr1*^{CreERT}*.Becn1*$^{flox/flox}$ mice. Next, the triple transgenic APPPS1.*Cx3cr1*^{CreERT}*.Becn1*$^{flox/flox}$ mice will be utilized to test our hypothesis in a disease model that already presents with neuroinflammation.

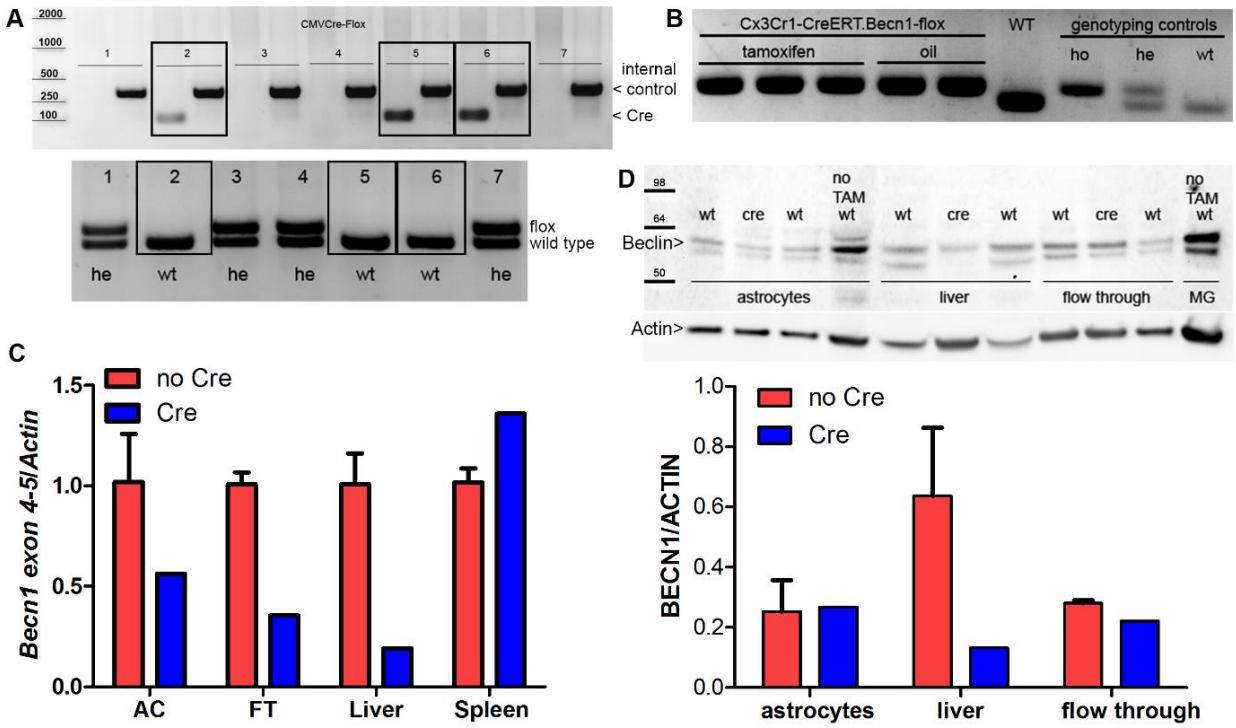

Figure 5. *in vivo* Cre-flox experiments
A) Genotyping of CMV^{Cre}.Becn1$^{flox/wt}$ mice. Mice #2, #5 and #6 are Cre positive. The genotyping for the lox site results in two bands for Cre negative mice, and only the lower wild type band for Cre positive mice, confirming the functionality of Cre dependent excision of the lox site. B) Genotyping of Cx3Cr1^{CreERT}.Becn1$^{flox/flox}$ mice treated either with tamoxifen or oil as a control. All mice show the band for the lox site, the tamoxifen did not induce Cre dependent excision. C) qPCR of tamoxifen treated Aldh1l1^{CreERT}.Becn1$^{flox/flox}$ mice. Decreased fold change for the lox flanked exons in the Aldh1l1 and Cre expressing cells. No Cre n=2, Cre n=1. D) Western blot of tamoxifen treated Aldh1l1^{CreERT}.Becn1$^{flox/flox}$ mice. Decreased BECN1 protein levels for liver cells. No Cre n=2, Cre n=1.

Astrocyte-specific knockdown of Becn1

In order to assess the role of BECN1 in yet another CNS glial cell type in neuroinflammation *in vivo* we investigated astrocytes. Astrocytes are known to be a modulator of neuroinflammatory processes and we hypothesized that decreasing autophagy specifically in these cells will increase neuroinflammation as well. We therefore tested this hypothesis by crossing the *Aldh1l1*^{CreERT} model (Winchenbach, Düking et al, 2016), specifically expressing Cre recombinase in astrocytes in the CNS, to the *Becn1*$^{flox/flox}$ mice.

Surprisingly, ten days after the tamoxifen injections the two mice treated with tamoxifen started to sicken and had to be sacrificed. When dissecting these mice, we noticed an enlarged and discolored liver, while other organs appeared normal. Lack of autophagy proteins in the liver is known to cause hepatomegaly (Komatsu, Waguri et al, 2005; Yoshii, Kuma et al, 2016), and *Aldh1l1* is expressed by ~80% of liver cells (Winchenbach, Düking et al, 2016). Although the hepatomegaly in *Atg5*$^{flox/flox}$ and *Atg7*$^{flox/flox}$ mice was not lethal, the *Becn1* deletion is still likely to be the cause of the observed serious symptoms of the *Aldh1l1*^{CreERT}*.Becn1*$^{flox/flox}$ mice. As mentioned before, BECN1 plays a role in more pathways than autophagy, and its importance in survival is demonstrated by the different lifespan of the complete knockout mice: while *Atg5* and *Atg7* knockout mice die in the neonatal stage (Komatsu, Waguri et al, 2005; Yoshii, Kuma et al, 2016), *Becn1* knockout mice do not survive beyond E7.5 (Yue, Jin et al, 2003).

To investigate whether tamoxifen could still induce an astrocyte-specific *Becn1* knockout in these ten days, we isolated astrocytes (see methods) for protein and gene expression analyses. Additionally, we prepared cell lysates from the liver and spleen as controls. qPCR analysis showed a strong reduction in the expression of *Becn1 exon 4-5* in the liver, as well as a reduced expression in the astrocytes, albeit not as strong as in the liver. The spleen samples served as a negative control, as there is no Aldh1l1 expression in spleen, consequently *Becn1 exon 4-5* expression was unchanged in spleen (Fig. 5C).

Next, we assessed BECN1 protein levels by means of western blot, this showed a similar pattern. A large reduction in BECN1 protein levels were found in the liver samples whilst a smaller reduction could be seen in astrocytes (Fig. 5D), in correspondence to the mRNA data. The difference in the targeting efficiency between the liver and astrocyte samples was unexpected, but could possibly be explained by the blood brain barrier, reducing the efficacy of reaching the astrocytes. Also, tamoxifen is metabolized in the liver hence the concentration of active tamoxifen is very high. Either way, due to the development of lethal hepatomegaly in *Aldh1l1*^{CreERT}*.Becn1*$^{flox/flox}$ mice, this model does not represent a good tool for assessing the role BECN1 in astrocytes. The only currently available alternative mouse model to target astrocytes is the GFAP-Cre model. Future studies could be approached with this tool, although one has to keep in mind that GFAP is also expressed by neuronal progenitors (Garcia, Doan et al, 2004).

CONCLUSION

For the first time, we could show the specific mechanism of autophagy-dependent cytokine release in microglia *in vitro*. *In vivo*, a constitutive partial knock down of *Becn1* in an AD-like model managed to affect the IL-1beta levels but failed to influence Abeta pathology. We are therefore generating a triple transgenic mouse model (*APPPS1.Cx3Cr1*^{CreERT}*.Becn1*$^{flox/flox}$ mice) enabling the specific analysis of microglial autophagy in an AD-like mouse model. This new tool and the generated knowledge will support a new direction of research, to unravel the therapeutic potential of autophagy-dependent inflammation in neurodegenerative diseases.

METHODS

Methods already described extensively in the paper are not repeated here.

Mice

To test the microglial-specific *Becn1* deletion in the *Cx3Cr1*^{CreERT}*.Becn1*$^{flox/flox}$ mice, 60-day-old animals were injected intraperitoneally with 75mg/kg tamoxifen diluted in olive oil, and a vehicle control group with just olive oil, for 5 consecutive days. To test the astrocyte-specific *Becn1* deletion in the *Aldh1l1*^{CreERT}*.Becn1*$^{flox/flox}$ mice the same treatment paradigm was applied. Animals were kept in individually ventilated cages with a 12 h light cycle with food and water *ad libitum*. All animal experiments were conducted in accordance with animal welfare acts and were approved by the regional office for health and social service in Berlin (LaGeSo), TVA G0251/15.

Cell isolation

Twenty days after the tamoxifen injections, we sacrificed the mice and isolated the cell populations of interest. From the *Cx3Cr1*^{CreERT}*.Becn1*$^{flox/flox}$ mice we isolated peritoneal macrophages, splenocytes, intestinal macrophages and microglia. Peritoneal macrophages were collected by peritoneal lavage with PBS. Splenocytes were collected from a spleen pressed through a 70µm cell strainer, treated with red blood cell lysis buffer and the cell suspension was enriched for CD11b+ cells with magnetic beads (Cat. 130-093-634, Miltenyi) according to manufacturers protocol. In short, the cell suspension is incubated with CD11b+ beads, and runs over a column attached to a magnet. CD11b+ cells stick to the column, while all other cells flow through. Afterwards, remove the column from the magnet and flush out the CD11b+ cells. Intestinal macrophages are collected by tissue lysis of the small intestine with collagenase IV (according to (Geem, Medina-Contreras et al, 2012)) and enriched for CD11b+ cells with magnetic beads (Cat. 130-093-634, Miltenyi). The hemispheres are dissociated using the neural tissue dissociation kit (Cat. 130-092-628, Miltenyi) and enriched for CD11b+ cells with magnetic beads (Cat. 130-093-634, Miltenyi). Microglia purity was assessed by FACS before further analysis (Fig. 6).

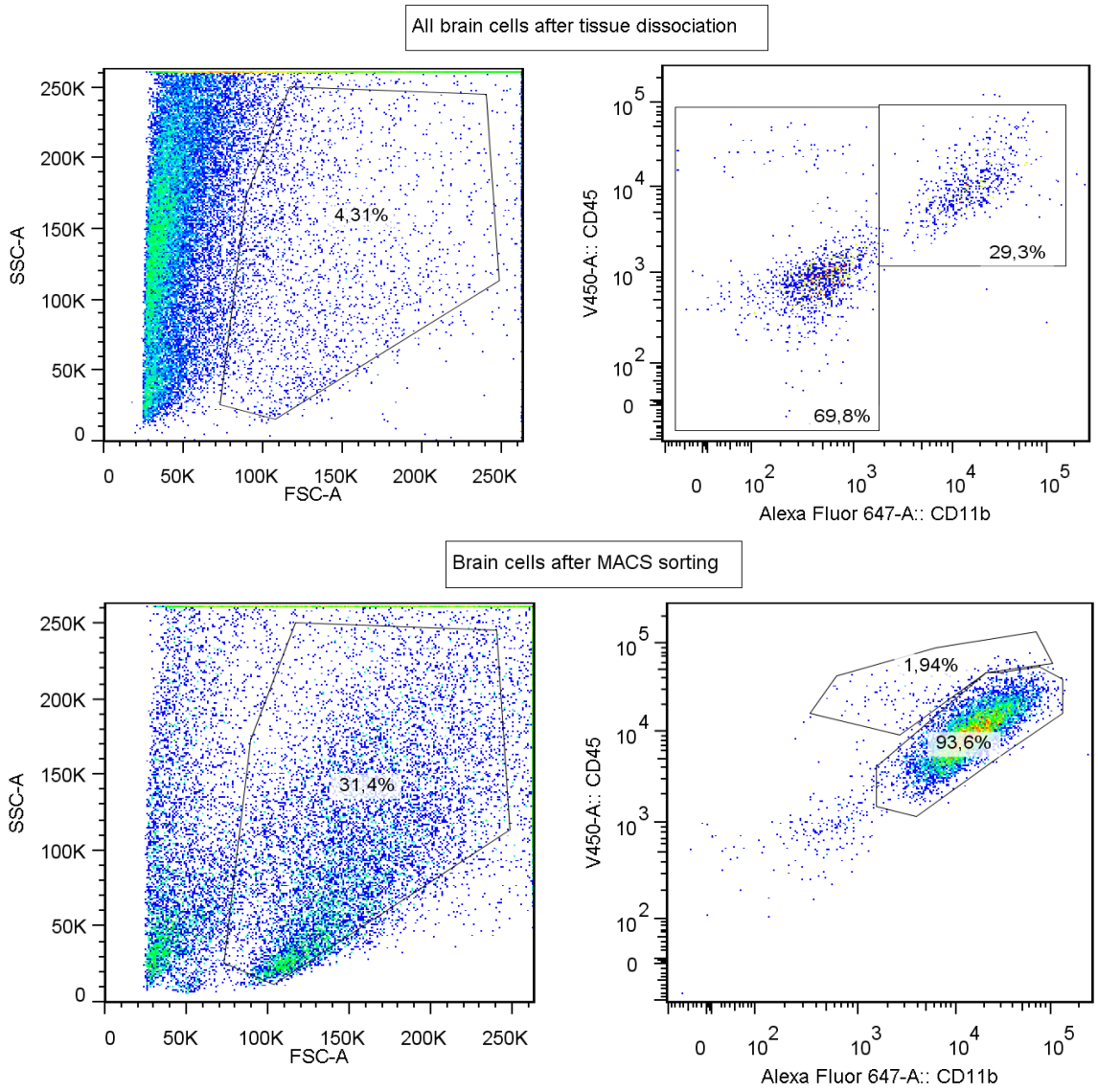

Figure 6. Purity check of microglia cell isolation with CD11b+ beads

Flow cytometry analysis of all brain cells before sorting with CD11b magnetic beads (top two graphs) and all brain cells after sorting with CD11b magnetic beads (bottom two graphs) from a 450 day old APPPS1 mouse with well-established Abeta pathology. MACS sorting purified the cell population to 93.6% microglia (CD11b+ CD45int) while 1.94% CNS-macrophages (CD11b+CD45hi) were found in the MACS sorted cell population.

From the *Aldh1l1*^{CreERT}*.Becn1*$^{flox/flox}$ mice we isolated astrocytes with the adult brain dissociation kit (Cat. 130-107-677, Miltenyi) including debris removal and red blood cell removal, followed by ACSA-2 magnetic beads sorting (Cat. 130-097-678, Miltenyi) over a column attached to a magnet. Here, the ACSA-2+ cells stick to the column, while all other cells flow through. Afterwards, the column is removed from the magnet and the astrocytes are flushed out.

Phagocytosis assay

We used an *in vitro* assay using fluorescent pHrodo *E. coli* bioparticles (Cat. P35361, Life Technologies) that are pH sensitive, and therefore emit light of a different wavelength when incorporated into lysosomes. The assay was performed according to the manufacturer's protocol. In short, plate cells in a 96 well plate and leave overnight, next day, replace medium by 100 µL bioparticles in culture medium [1 mg/mL]. Incubate cells with the bioparticles for 1 hour in a 37C incubator without CO_2. Fluorescence is measured with a fluorescent microplate reader (iControl software, Tecan). Auto-fluorescence is corrected by a medium-only control measurement. Phagocytic capacity is normalized to non-treated cells, and a negative control of Cytochalasin D (C2618-200UL, Sigma) treated cells is always included.

Primer design

To assess the deletion of exon 4-7 of the *Becn1* gene specifically, we designed SybrGreen qPCR primers bridging exon 4 and exon 5, using the ApE software to select the respective DNA sequence and NCBI/Primer blast to verify the complementarity and GC balance. We confirmed the melting curve was clean and that the qPCR product on an electrophoresis gel had the expected size (116 bp).

Primer sequences:

Forward primer Becn1_exon4-5	ACCCGCTGTGTGAGGAATG
Reverse primer Becn1_exon4-5	CATCTGCTCTAGGATCTCCAAACA

Immunoprecipitation

One million microglia were plated in a well of a 6 well plate and stimulated with LPS/ATP or not stimulated at all. These were harvested and collected as a pellet. The pellet was used to perform the immunoprecipitation according to the manufacturer's protocol. In short, lyse the cell pellet and incubate with protein A/G agarose suspension for 3 hours. 1 hour incubation with the antibody followed by overnight incubation with protein A/G agarose suspension. Perform 5 washes with 3 different wash buffers to obtain the final protein pellet for western blot. A sample was taken from the lysed cell pellet before incubation with A/G agarose suspension as a control. For western blot method see manuscript.

REFERENCES

Bennett FC, Bennett ML, Yaqoob F, Mulinyawe SB, Grant GA, Hayden Gephart M, Plowey ED, Barres BA (2018) A Combination of Ontogeny and CNS Environment Establishes Microglial Identity. *Neuron* **98:** 1170-1183.e1178

Cho M-H, Cho K, Kang H-J, Jeon E-Y, Kim H-S, Kwon H-J, Kim H-M, Kim D-H, Yoon S-Y (2014) Autophagy in microglia degrades extracellular β-amyloid fibrils and regulates the NLRP3 inflammasome. *Autophagy* **10:** 1761-1775

Das A, Kim SH, Arifuzzaman S, Yoon T, Chai JC, Lee YS, Park KS, Jung KH, Chai YG (2016) Transcriptome sequencing reveals that LPS-triggered transcriptional responses in established microglia BV2 cell lines are poorly representative of primary microglia. *Journal of Neuroinflammation* **13:** 182

François A, Terro F, Janet T, Bilan AR, Paccalin M, Page G (2013) Involvement of interleukin-1β in the autophagic process of microglia: relevance to Alzheimer's disease. *Journal of Neuroinflammation* **10:** 915

Furuya N, Kakuta S, Sumiyoshi K, Ando M, Nonaka R, Suzuki A, Kazuno S, Saiki S, Hattori N (2018) NDP52 interacts with mitochondrial RNA poly(A) polymerase to promote mitophagy. *EMBO reports*

Garcia ADR, Doan NB, Imura T, Bush TG, Sofroniew MV (2004) GFAP-expressing progenitors are the principal source of constitutive neurogenesis in adult mouse forebrain. *Nature Neuroscience* **7:** 1233

Geem D, Medina-Contreras O, Kim W, Huang CS, Denning TL (2012) Isolation and Characterization of Dendritic Cells and Macrophages from the Mouse Intestine. *JoVE***:** e4040

Ginhoux F, Greter M, Leboeuf M, Nandi S, See P, Gokhan S, Mehler MF, Conway SJ, Ng LG, Stanley ER, Samokhvalov IM, Merad M (2010) Fate Mapping Analysis Reveals That Adult Microglia Derive from Primitive Macrophages. *Science* **330:** 841-845

Heppner FL, Ransohoff RM, Becher B (2015) Immune attack: the role of inflammation in Alzheimer disease. *Nature Reviews Neuroscience* **16:** 358

Hickman SE, Kingery ND, Ohsumi TK, Borowsky ML, Wang L-c, Means TK, El Khoury J (2013) The microglial sensome revealed by direct RNA sequencing. *Nature Neuroscience* **16:** 1896

Houtman J, Freitag K, Gimber N, Schmoranzer J, Heppner FL, Jendrach M (2019) Beclin1-driven autophagy modulates the inflammatory response of microglia via NLRP3. *The EMBO Journal* **38**

Inomata M, Into T (2012) Nuclear dot protein 52, an autophagy-associated protein, regulates Toll-like receptor signaling. *Journal of Oral Biosciences* **54:** 151-154

Jo C, Gundemir S, Pritchard S, Jin YN, Rahman I, Johnson GVW (2014) Nrf2 reduces levels of phosphorylated tau protein by inducing autophagy adaptor protein NDP52. *Nature Communications* **5:** 3496

Kaartinen V, Nagy A (2001) Removal of the floxed neo gene from a conditional knockout allele by the adenoviral Cre recombinase in vivo. *genesis* **31:** 126-129

Kim S, Lee D, Song JC, Cho S-J, Yun S-M, Koh YH, Song J, Johnson GVW, Jo C (2014) NDP52 associates with phosphorylated tau in brains of an Alzheimer disease mouse model. *Biochemical and Biophysical Research Communications* **454:** 196-201

Komatsu M, Waguri S, Ueno T, Iwata J, Murata S, Tanida I, Ezaki J, Mizushima N, Ohsumi Y, Uchiyama Y, Kominami E, Tanaka K, Chiba T (2005) Impairment of starvation-induced and constitutive autophagy in Atg7-deficient mice. *The Journal of Cell Biology* **169:** 425-434

Krabbe G, Halle A, Matyash V, Rinnenthal JL, Eom GD, Bernhardt U, Miller KR, Prokop S, Kettenmann H, Heppner FL (2013) Functional Impairment of Microglia Coincides with Beta-Amyloid Deposition in Mice with Alzheimer-Like Pathology. *PLOS ONE* **8:** e60921

Krstic D, Madhusudan A, Doehner J, Vogel P, Notter T, Imhof C, Manalastas A, Hilfiker M, Pfister S, Schwerdel C, Riether C, Meyer U, Knuesel I (2012) Systemic immune challenges trigger and drive Alzheimer-like neuropathology in mice. *Journal of Neuroinflammation* **9:** 151

Lee H-Y, Kim J, Quan W, Lee J-C, Kim M-S, Kim S-H, Bae J-W, Hur KY, Lee M-S (2016) Autophagy deficiency in myeloid cells increases susceptibility to obesity-induced diabetes and experimental colitis. *Autophagy* **12:** 1390-1403

Lodder J, Denaës T, Chobert M-N, Wan J, El-Benna J, Pawlotsky J-M, Lotersztajn S, Teixeira-Clerc F (2015) Macrophage autophagy protects against liver fibrosis in mice. *Autophagy* **11:** 1280-1292

Lucin Kurt M, O'Brien Caitlin E, Bieri G, Czirr E, Mosher Kira I, Abbey Rachelle J, Mastroeni Diego F, Rogers J, Spencer B, Masliah E, Wyss-Coray T (2013) Microglial Beclin 1 Regulates Retromer Trafficking and Phagocytosis and Is Impaired in Alzheimer's Disease. *Neuron* **79:** 873-886

Menzies FM, Fleming A, Rubinsztein DC (2015) Compromised autophagy and neurodegenerative diseases. *Nature Reviews Neuroscience* **16:** 345

Montine TJ, Phelps CH, Beach TG, Bigio EH, Cairns NJ, Dickson DW, Duyckaerts C, Frosch MP, Masliah E, Mirra SS, Nelson PT, Schneider JA, Thal DR, Trojanowski JQ, Vinters HV, Hyman BT (2012) National Institute on Aging–Alzheimer's Association guidelines for the neuropathologic assessment of Alzheimer's disease: a practical approach. *Acta Neuropathologica* **123:** 1-11

O'Brien CE, Bonanno L, Zhang H, Wyss-Coray T (2015) Beclin 1 regulates neuronal transforming growth factor-β signaling by mediating recycling of the type I receptor ALK5. *Molecular Neurodegeneration* **10:** 69

Pickford F, Masliah E, Britschgi M, Lucin K, Narasimhan R, Jaeger PA, Small S, Spencer B, Rockenstein E, Levine B, Wyss-Coray T (2008) The autophagy-related protein beclin 1 shows reduced expression in early Alzheimer disease and regulates amyloid beta accumulation in mice. *The Journal of clinical investigation* **118:** 2190-2199

Qu X, Yu J, Bhagat G, Furuya N, Hibshoosh H, Troxel A, Rosen J, Eskelinen E-L, Mizushima N, Ohsumi Y, Cattoretti G, Levine B (2003) Promotion of tumorigenesis by heterozygous disruption of the beclin 1 autophagy gene. *The Journal of Clinical Investigation* **112:** 1809-1820

Querfurth HW, LaFerla FM (2010) Alzheimer's Disease. *New England Journal of Medicine* **362:** 329-344

Radde R, Bolmont T, Kaeser SA, Coomaraswamy J, Lindau D, Stoltze L, Calhoun ME, Jäggi F, Wolburg H, Gengler S, Haass C, Ghetti B, Czech C, Hölscher C, Mathews PM, Jucker M (2006) Abeta42-driven cerebral amyloidosis in transgenic mice reveals early and robust pathology. *EMBO reports* **7:** 940-946

Rockenstein E, Mallory M, Mante M, Sisk A, Masliaha E (2001) Early formation of mature amyloid-β protein deposits in a mutant APP transgenic model depends on levels of Aβ1–42. *Journal of Neuroscience Research* **66:** 573-582

Saitoh T, Fujita N, Jang MH, Uematsu S, Yang B-G, Satoh T, Omori H, Noda T, Yamamoto N, Komatsu M, Tanaka K, Kawai T, Tsujimura T, Takeuchi O, Yoshimori T, Akira S (2008) Loss of the autophagy protein Atg16L1 enhances endotoxin-induced IL-1β production. *Nature* **456:** 264

Suzuki K, Kubota Y, Sekito T, Ohsumi Y (2007) Hierarchy of Atg proteins in pre-autophagosomal structure organization. *Genes to Cells* **12:** 209-218

Tumbarello DA, Manna PT, Allen M, Bycroft M, Arden SD, Kendrick-Jones J, Buss F (2015) The Autophagy Receptor TAX1BP1 and the Molecular Motor Myosin VI Are Required for Clearance of Salmonella Typhimurium by Autophagy. *PLOS Pathogens* **11:** e1005174

von Muhlinen N, Akutsu M, Ravenhill Benjamin J, Foeglein Á, Bloor S, Rutherford Trevor J, Freund Stefan MV, Komander D, Randow F (2012) LC3C, Bound Selectively by a Noncanonical LIR Motif in NDP52, Is Required for Antibacterial Autophagy. *Molecular Cell* **48:** 329-342

Walsh JG, Muruve DA, Power C (2014) Inflammasomes in the CNS. *Nature Reviews Neuroscience* **15:** 84

Weber A, Wasiliew P, Kracht M (2010) Interleukin-1 (IL-1) Pathway. *Science Signaling* **3:** cm1-cm1

Winchenbach J, Düking T, Berghoff S, Stumpf S, Hülsmann S, Nave K, Saher G (2016) Inducible targeting of CNS astrocytes in Aldh1l1-CreERT2 BAC transgenic mice [version 1; referees: 3 approved]. *F1000Research* **5**

Yang C, Kaushal V, Shah SV, Kaushal GP (2008) Autophagy is associated with apoptosis in cisplatin injury to renal tubular epithelial cells. *American Journal of Physiology-Renal Physiology* **294:** F777-F787

Yang Y, Wang G, Huang X, Du Z (2015) Crystallographic and modelling studies suggest that the SKICH domains from different protein families share a common Ig-like fold but harbour substantial structural variations. *Journal of Biomolecular Structure and Dynamics* **33:** 1385-1398

Ye J, Jiang Z, Chen X, Liu M, Li J, Liu N (2017) The role of autophagy in pro-inflammatory responses of microglia activation via mitochondrial reactive oxygen species in vitro. *Journal of Neurochemistry* **142:** 215-230

Yona S, Kim K-W, Wolf Y, Mildner A, Varol D, Breker M, Strauss-Ayali D, Viukov S, Guilliams M, Misharin A, Hume David A, Perlman H, Malissen B, Zelzer E, Jung S (2013) Fate Mapping Reveals Origins and Dynamics of Monocytes and Tissue Macrophages under Homeostasis. *Immunity* **38:** 79-91

Yoshii Saori R, Kuma A, Akashi T, Hara T, Yamamoto A, Kurikawa Y, Itakura E, Tsukamoto S, Shitara H, Eishi Y, Mizushima N (2016) Systemic Analysis of Atg5-Null Mice Rescued from Neonatal Lethality by Transgenic ATG5 Expression in Neurons. *Developmental Cell* **39:** 116-130

Yue Z, Jin S, Yang C, Levine AJ, Heintz N (2003) Beclin 1, an autophagy gene essential for early embryonic development, is a haploinsufficient tumor suppressor. *Proceedings of the National Academy of Sciences* **100:** 15077-15082

Eidesstattliche Versicherung

„Ich, Judith Houtman, versichere an Eides statt durch meine eigenhändige Unterschrift, dass ich die vorgelegte Dissertation mit dem Thema: ‚Autophagy in microglia and Alzheimer's disease' selbstständig und ohne nicht offengelegte Hilfe Dritter verfasst und keine anderen als die angegebenen Quellen und Hilfsmittel genutzt habe.
Alle Stellen, die wörtlich oder dem Sinne nach auf Publikationen oder Vorträgen anderer Autoren beruhen, sind als solche in korrekter Zitierung (siehe „Uniform Requirements for Manuscripts (URM)" des ICMJE -*www.**icmje**.org*) kenntlich gemacht. Die Abschnitte zu Methodik (insbesondere praktische Arbeiten, Laborbestimmungen, statistische Aufarbeitung) und Resultaten (insbesondere Abbildungen, Graphiken und Tabellen) entsprechen den URM (s.o) und werden von mir verantwortet.
Mein Anteil an der ausgewählten Publikation entspricht dem, der in der untenstehenden gemeinsamen Erklärung mit dem/der Betreuer/in, angegeben ist. Sämtliche Publikationen, die aus dieser Dissertation hervorgegangen sind und bei denen ich Autor bin, entsprechen den URM (s.o) und werden von mir verantwortet.
Die Bedeutung dieser eidesstattlichen Versicherung und die strafrechtlichen Folgen einer unwahren eidesstattlichen Versicherung (§156,161 des Strafgesetzbuches) sind mir bekannt und bewusst."

Datum _____ Unterschrift

Ausführliche Anteilserklärung an der erfolgten Publikation

[Die Anteile an der ausgewählten Publikation sind so deutlich und detailliert zu erklären, dass es der Promotionskommission und den wissenschaftlichen Gutachtern ohne Probleme möglich ist zu erkennen, was Sie selbst dazu beigetragen haben. Wünschenswert wäre ein konkreter Bezug zur Publikation selbst wie z. B.: „aus meiner statistischen Auswertung sind die Tabellen 1, 4, 47 und 60 entstanden."

Publikation 1: [2019]
Judith Houtman[1], Kiara Freitag[1 4], Niclas Gimber[2], Jan Schmoranzer[2], Frank L. Heppner[1 3 4 #], Marina Jendrach [1 #], Beclin1-driven autophagy modulates the inflammatory response of microglia via NLRP3, The EMBO Journal, 32/3, 2019

Beitrag im Einzelnen:
Alle Mäuse wurden von mir gezüchtet und getötet. Die Perfusion sowie die Organ- / Zellisolation von erwachsenen Mäusen wurde von mir durchgeführt. Die Weiterverarbeitung des Gehirns für Abeta und proinflammatorischen ELISA wurde von mir und Kiara Freitag durchgeführt (Fig. 2, EV1). Alle Phagozytose Assays, Färbungen und Quantifizierungen von Abeta wurden von mir durchgeführt (Fig. EV2). Die siRNA KD von CALCOCO-2 wurde von mir durchgeführt (Fig. 5). Färbungen von adulten Mikroglia wurden von mir durchgeführt (Fig. EV5). Zellkulturexperimente, Western Blots, Mikroskopie und statistische Auswertungen sind in Zusammenarbeit mit Kiara Freitag und Marina Jendrach entstanden (Fig. 1, 2, 3, 4).

_____
Unterschrift, Datum und Stempel des betreuenden Hochschullehrers/der betreuenden Hochschullehrerin

_____
Unterschrift des Doktoranden/der Doktorandin

Journal summary list

Journal Data Filtered By: **Selected JCR Year: 2017** Selected Editions: SCIE,SSCI
Selected Categories: **"CELL BIOLOGY"** Selected Category Scheme: WoS
Gesamtanzahl: 190 Journale

Rank	Full Journal Title	Total Cites	Journal Impact Factor	Eigenfactor Score
1	NATURE REVIEWS MOLECULAR CELL BIOLOGY	43,667	35.612	0.095540
2	NATURE MEDICINE	75,461	32.621	0.171980
3	CELL	230,625	31.398	0.583260
4	Cell Stem Cell	23,493	23.290	0.096030
5	CANCER CELL	35,217	22.844	0.096910
6	Cell Metabolism	29,834	20.565	0.101740
7	NATURE CELL BIOLOGY	39,896	19.064	0.092960
8	TRENDS IN CELL BIOLOGY	13,708	18.564	0.037630
9	Science Translational Medicine	26,691	16.710	0.126450
10	CELL RESEARCH	13,728	15.393	0.037450
11	MOLECULAR CELL	61,604	14.248	0.181170
12	NATURE STRUCTURAL & MOLECULAR BIOLOGY	27,547	13.333	0.081820
13	Autophagy	14,923	11.100	0.035510
14	TRENDS IN MOLECULAR MEDICINE	9,213	11.021	0.019720
15	EMBO JOURNAL	67,036	10.557	0.079780
16	CURRENT OPINION IN CELL BIOLOGY	13,339	10.015	0.027790
17	DEVELOPMENTAL CELL	26,896	9.616	0.074980
18	GENES & DEVELOPMENT	57,469	9.462	0.092720
19	CURRENT BIOLOGY	56,595	9.251	0.137200
20	Cold Spring Harbor Perspectives in Biology	13,275	9.247	0.049360
21	Annual Review of Cell and Developmental Biology	9,812	9.032	0.016870
22	Cell Systems	1,129	8.982	0.009600
23	AGEING RESEARCH REVIEWS	5,297	8.973	0.012030
24	JOURNAL OF CELL BIOLOGY	68,915	8.784	0.085170
25	EMBO REPORTS	13,293	8.749	0.031350
26	PLANT CELL	48,393	8.228	0.063640
27	MATRIX BIOLOGY	4,803	8.136	0.008500
28	Cell Reports	29,789	8.032	0.210690

1

Selected JCR Year: 2017; Selected Categories: "CELL BIOLOGY"

Published online: January 7, 2019

Article

SOURCE DATA | TRANSPARENT PROCESS

THE EMBO JOURNAL

Beclin1-driven autophagy modulates the inflammatory response of microglia via NLRP3

Judith Houtman[1], Kiara Freitag[1,2], Niclas Gimber[3], Jan Schmoranzer[3], Frank L Heppner[1,2,4,†] & Marina Jendrach[1,*,†]

Abstract

Alzheimer's disease is characterized not only by extracellular amyloid plaques and neurofibrillary tangles, but also by microglia-mediated neuroinflammation. Recently, autophagy has been linked to the regulation of the inflammatory response. Thus, we investigated how an impairment of autophagy mediated by BECN1/Beclin1 reduction, as described in Alzheimer's disease patients, would influence cytokine production of microglia. Acutely stimulated microglia from *Becn1*$^{+/-}$ mice exhibited increased expression of IL-1beta and IL-18 compared to wild-type microglia. *Becn1*$^{+/-}$ *APPPS1* mice also contained enhanced IL-1beta levels. The investigation of the IL-1beta/IL-18 processing pathway showed an elevated number of cells with inflammasomes and increased levels of NLRP3 and cleaved CASP1/Caspase1 in *Becn1*$^{+/-}$ microglia. Super-resolation microscopy revealed a very close association of NLRP3 aggregates and LC3-positive vesicles. Interestingly, CALCOCO2 colocalized with NLRP3 and its downregulation increased IL-1beta release. These data support the notion that selective autophagy can impact microglia activation by modulating IL-1beta and IL-18 production via NLRP3 degradation and thus present a mechanism how impaired autophagy could contribute to neuroinflammation in Alzheimer's disease.

Keywords Alzheimer's disease; autophagy; BECN1/Beclin1; inflammation; microglia

Subject Categories Immunology; Neuroscience

DOI 10.15252/embj.201899430 | Received 15 March 2018 | Revised 28 November 2018 | Accepted 5 December 2018

The EMBO Journal (2019) e99430

Introduction

Alzheimer's disease (AD) is the most common neurodegenerative disorder. The main hallmarks of AD are extracellular amyloid plaques (main component amyloid-beta (Abeta) peptide), neurofibrillary tangles (the main component hyperphosphorylated MAP tau), and neuroinflammation. Microglia, the resident immune cells of the central nervous system, are involved in two aspects of AD: removal of extracellular Abeta by phagocytosis and production and release of cytokines resulting in progressive neuroinflammation. Neuroinflammation correlates in many animal models with an increase in extracellular Abeta, and microglia are regarded as the main producers of pro-inflammatory cytokines (Heppner *et al*, 2015). *In vivo* interleukin (IL)-1 (Griffin *et al*, 1989), IL-6, granulocyte-macrophage colony-stimulating factor (GM-CSF) (Patel *et al*, 2005), IL-12, and IL-23 (Vom Berg *et al*, 2012), as well as tumor necrosis factor (TNF) alpha (Fillit *et al*, 1991), were detected in human patients with AD or in different animal models with AD-like pathology (Prokop *et al*, 2013). While enhanced neuroinflammation is well established in the late stages of AD, recent data also suggest a role for inflammation in the development of the disease. Injection of double-stranded RNA (Poly:IC) into wild-type mice, thus mimicking viral infection, resulted in increased IL-1beta levels followed by an AD-like pathology at higher age (Krstic *et al*, 2012). Furthermore, mouse models lacking the pro-IL-1beta processing proteins NLRP3 (NLR family, pyrin domain containing 3) or CASP1/Caspase1 show decreased inflammation and Abeta burden and increased Abeta phagocytosis (Heneka *et al*, 2013).

The mechanisms behind enhanced microglial activation and increased cytokine release in AD seem to be diverse. Priming of microglia by interaction with Abeta is a possibility (Heppner *et al*, 2015). Another or additional mechanism could be autophagy, as recent work on myeloid cells indicates that impaired autophagy mediates increased inflammation. Mutations in the AD risk factor TREM2 are linked to anomalous autophagy (Ulland *et al*, 2017). Loss of the autophagy protein ATG16L1 is associated with Crohn's disease and resulted in enhanced pro-inflammatory cytokine production of macrophages in response to stress (Saitoh *et al*, 2008; Murthy *et al*, 2014). A conditional knock-out of *Atg5* or *Atg7* in macrophages correlated with increased severity of uveitis (Santeford

1 Department of Neuropathology, Charité – Universitätsmedizin Berlin, corporate member of Freie Universität Berlin, Humboldt-Universität zu Berlin, Berlin Institute of Health, Berlin, Germany
2 German Center for Neurodegenerative Diseases (DZNE) within the Helmholtz Association, Berlin, Germany
3 Core Facility Advanced Medical Bioimaging (AMBIO), Charité – Universitätsmedizin Berlin, corporate member of Freie Universität Berlin, Humboldt-Universität zu Berlin, Berlin Institute of Health, Berlin, Germany
4 Cluster of Excellence, NeuroCure, Berlin, Germany
*Corresponding author. Tel: +49 30 450536291; E-mail: marina.jendrach@charite.de
†These authors contributed equally to this work

© 2019 The Authors

et al, 2016), liver fibrosis (Lodder *et al*, 2015), or colitis (Lee *et al*, 2016). *In vitro* data on macrophages and macrophage cell lines show that addition of the autophagy blocker 3-MA resulted in increased IL-1beta formation (Harris *et al*, 2011; Zhou *et al*, 2011; Shi *et al*, 2012; de Luca *et al*, 2014). Data on microglia are emerging but are somewhat controversial: Some publications describe increased activation of primary mouse microglia or the microglial cell line BV2 after knockdown of autophagy genes (Cho *et al*, 2014; Ye *et al*, 2017) or lysosomal damage by manganese (Wang *et al*, 2017). Others have reported no changes in cytokine release when autophagic flux was blocked for 24 h by Bafilomycin A1 (François *et al*, 2013).

Microglia isolated from human AD patients show strongly reduced protein levels of BECN1/Beclin1 (Lucin *et al*, 2013). BECN1 is an essential part of the multi-protein complex that is necessary for nucleation of the autophagic vesicle (Zhang *et al*, 2016). Homozygous loss of *Becn1* causes embryonic cell death between E7.5 and E8.5 (Yue *et al*, 2003), while heterozygous loss of *Becn1* mediates decreased autophagy in different cell types (Qu *et al*, 2003; Pickford *et al*, 2008). Furthermore, heterozygous loss of *Becn1* in an AD mouse model (T41 $APP^{+/-}$ mice) resulted in increased Abeta burden (Pickford *et al*, 2008). In addition, BECN1 was shown to be involved in receptor recycling and retromer recruitment in phagocytosis of Abeta *in vitro* (Lucin *et al*, 2013).

Based on these data, we envision a central role for microglial BECN1 in the regulation of neuroinflammation.

Results

Reduction in BECN1 and impairment of autophagy results in enhanced IL-1beta and IL-18 release from microglia

To investigate whether modulation of BECN1 levels in microglia influences neuroinflammatory responses, $Becn1^{+/-}$ mice were chosen as a model system with reduced BECN1 levels. The use of *Becn1* heterozygous mice was necessary since $Becn1^{-/-}$ mice die *in utero* before the microglia precursor cells leave the yolk sac to colonize the developing brain (Yue *et al*, 2003). Microglia were isolated from newborn $Becn1^{+/-}$ and wild-type mouse pups. The BECN1 content of microglia from $Becn1^{+/-}$ and wild-type mice was assessed by Western blotting: Microglia from $Becn1^{+/-}$ mice show around 50% reduction in BECN1 protein compared to microglia from wild-type mice (Fig 1A). Next, the effect of BECN1 reduction on autophagy was determined. Microglia were kept for 2 h either in cultivation medium (DMEM with 10% FCS) or in amino acid-free starvation medium (HBSS), in the presence or absence of Bafilomycin A1. While the HBSS-cultured microglia showed a trend of decreased autophagic flux in the Bafilomycin A1-treated $Becn1^{+/-}$ microglia, LC3-II/MAP1LC3B-II levels of $Becn1^{+/-}$ microglia were significantly lower when autophagic flux was blocked with Bafilomycin A1 in medium-exposed cells, in accordance with the reduced BECN1 content (Fig 1B). Staining of endogenous LC3-positive vesicles in Bafilomycin A1-treated microglia supports these data (Fig 1C).

To determine the effect of BECN1 and autophagy reduction on inflammation, microglia were treated with a standard acute pro-inflammatory stimulus: Cells were subjected for 3 h to LPS (1 μg/ml) followed by 45 min of ATP (1 mM). To quantify the release of pro-inflammatory cytokines, AD-relevant cytokines IL-1beta, IL-18, TNFalpha, and IL-6 were measured by ELISA. Reduction in BECN1 resulted in an increased presence of IL-1beta and IL-18 in the supernatant of LPS/ATP-stimulated $Becn1^{+/-}$ microglia compared to the supernatant of LPS/ATP-stimulated wild-type microglia (Fig 2A and B). Increased IL-1beta levels were also detected in the supernatant of $Becn1^{+/-}$ microglia by Western blot (Fig EV1A). In contrast, levels of TNFalpha and IL-6 were not altered (Fig EV1B).

Subsequently, we sought to confirm these data by a pharmacological approach: Microglia isolated from wild-type mouse pups were treated with the pro-inflammatory stimulus in growth medium with 10% FCS or in amino acid-free starvation medium HBSS. IL-1beta release after stimulation with LPS/ATP was significantly lower in cells kept in HBSS (Fig 2C). Furthermore, wild-type microglia in full medium or HBSS were stimulated with LPS and ATP in the presence or absence of the autophagy blocker 3-Methyladenine (3-MA). Short-term treatment of 3-MA for 1 h 45 min resulted in reduction in LC3-positive vesicles (Fig 2D) and in a significant increase in IL-1beta (Fig 2C). While cells kept in HBSS released less cytokines in general, TNFalpha release was decreased upon 3-MA treatment in growth medium as well as in HBSS medium, whereas the IL-6 release was not affected by 3-MA treatment (Fig EV1C).

To investigate whether reduced BECN1 levels also have an effect on inflammation *in vivo*, we crossed $Becn1^{+/-}$ mice to *APPPS1* mice. *APPPS1* mice are an established AD model with progressive amyloid-beta pathology and corresponding neuroinflammation (Radde *et al*, 2006). *APPPS1* $Becn1^{+/-}$ mice were analyzed at 3 months (amyloid-beta deposits detectable in the brain), 4 months

Figure 1. Autophagy is impaired in $Becn1^{+/-}$ microglia.

A BECN1 expression of microglia from $Becn1^{+/-}$ and wild-type mouse pups in full medium without Bafilomycin A1 (Baf) was quantified by Western blotting. Microglia from $Becn1^{+/-}$ mice show a significant reduction in BECN1 (48%) compared to microglia from wild-type mice; mean ± SEM, wild-type $n = 3$, $Becn1^{+/-}$ $n = 7$; two-tailed *t*-test $^{**}P < 0.01$. Blot shows representative amounts of BECN1 after various treatments.

B Microglia from newborn $Becn1^{+/-}$ and wild-type mouse pups were kept for 2 h either in full medium or in HBSS with or without Bafilomycin A1 (Baf). LC3 and ACTIN levels were determined by Western blot. LC3-II was significantly reduced in microglia from $Becn1^{+/-}$ mice after Baf treatment in full medium compared to wild-type microglia; mean ± SEM, wild-type $n = 3$, $Becn1^{+/-}$ $n = 4$; two-tailed *t*-test $^{*}P < 0.05$.

C Microglia from newborn $Becn1^{+/-}$ and wild-type mouse pups were kept for 2 h either in full medium or HBSS with Bafilomycin A1 (Baf) and stained for endogenous LC3. Exemplary images and the quantification of LC3-positive vesicles/μm^2 cell area show reduced presence of LC3-positive vesicles in microglia from $Becn1^{+/-}$ mice and induction of autophagy by HBSS; mean ± SEM, wild-type $n = 4$, $Becn1^{+/-}$ $n = 4$, 3–5 fields per view/*n* and condition and 73–271 cells/*n* and condition; two-tailed *t*-test $^{*}P < 0.05$; scale bar: 20 μm.

Source data are available online for this figure.

© 2019 The Authors

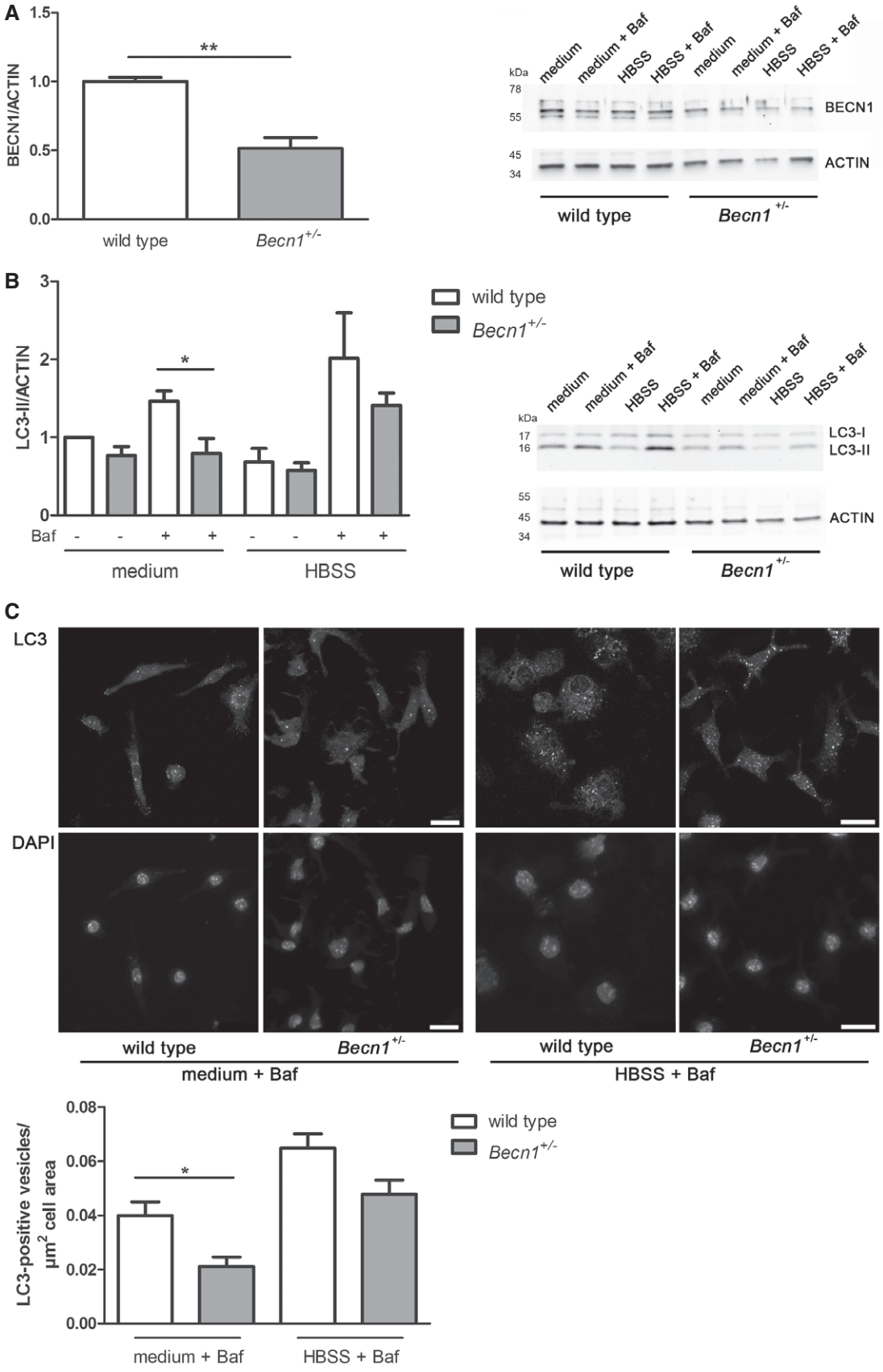
A
BECN1/ACTIN
1.5
1.0
0.5
0.0
**
wild type
Becn1+/-
kDa
78
55
45
34
medium
medium + Baf
HBSS
HBSS + Baf
BECN1
ACTIN
wild type
Becn1+/-
B
LC3-II/ACTIN
3
2
1
0
*
Baf
medium
HBSS
wild type
Becn1+/-
17
16
LC3-I
LC3-II
C
LC3
DAPI
wild type
Becn1+/-
medium + Baf
HBSS + Baf
LC3-positive vesicles/ µm2 cell area
0.08
0.06
0.04
0.02
0.00

Figure 1.

Figure 2. Reduction in BECN1 results in enhanced IL-1beta and IL-18 release.

A, B Microglia isolated from newborn *Becn1*$^{+/-}$ and wild-type mouse pups were either non treated or treated with a pro-inflammatory stimulus (LPS followed by ATP). As additional controls, cells treated only with LPS or ATP were used in (A). The concentration of the pro-inflammatory cytokines IL-1beta (A) and IL-18 (B) in the cell supernatant was determined by ELISA. Reduction in BECN1 significantly enhanced release of both cytokines after stimulation with LPS/ATP; mean ± SEM, wild-type *n* (A/B) = 9/2, wild-type LPS *n* = 3/0, wild-type ATP *n* = 3/0, wild-type LPS/ATP *n* = 9/9, *Becn1*$^{+/-}$ *n* = 23/5, *Becn1*$^{+/-}$ LPS/ATP *n* = 23/23, two-tailed *t*-test *$P < 0.05$.

C Microglia isolated from wild-type mouse pups were pre-incubated in full medium or starvation medium HBSS before addition of a pro-inflammatory stimulus (LPS followed by ATP). The autophagy blocker 3-MA was added for the final 1 h 45 min of the experiment. The concentration of the pro-inflammatory cytokine IL-1beta in the cell supernatant was determined by ELISA. Incubation with HBSS reduced IL-1beta release significantly while 3-MA treatment increased it; mean ± SEM, full medium *n* = 6, full medium LPS/ATP *n* = 6, full medium LPS/ATP + 3-MA *n* = 3, HBSS *n* = 6, HBSS LPS/ATP *n* = 6, HBSS LPS/ATP + 3-MA *n* = 6; two-tailed *t*-test *$P < 0.05$; **$P < 0.01$.

D Microglia isolated from wild-type mouse pups were pre-incubated in starvation medium HBSS before addition of a pro-inflammatory stimulus (LPS followed by ATP). The autophagy blocker 3-MA was added for the final 1 h 45 min of the experiment, microglia were stained for LC3, and images were taken by confocal microscopy. Representative images show a reduction in LC3-positive vesicles in 3-MA-treated cells. Scale bar: 20 μm.

E Proteins were extracted from brains of wild-type, *Becn1*$^{+/-}$, *APPPS1*, and *APPPS1 Becn1*$^{+/-}$ mice at the indicated ages. IL-1beta was measured by electrochemiluminescence (Meso Scale) and compared within the respective age groups. IL-1beta was significantly increased in the TBS and TX fraction; mean ± SEM, wild-type: *n* (per age group) = 2/6/3, *Becn1*$^{+/-}$: *n* = 2/5/2, *APPPS1*: *n* = 5/5/6, *APPPS1 Becn1*$^{+/-}$: *n* = 7/9/6; ANOVA with Dunnett's *post hoc* test with WT as control group; *$P < 0.05$; **$P < 0.01$.

F Proteins were extracted from brains of *APPPS1* and of *APPPS1 Becn1*$^{+/-}$ mice at the indicated ages. Amyloid-beta 1-40 and 1-42 were measured by electrochemiluminescence (Meso Scale) and compared within the respective age groups. No difference in the amyloid-beta load between the genotypes is apparent; mean ± SEM, *APPPS1*: *n* = 5/5/6, *APPPS1 Becn1*$^{+/-}$: *n* = 7/9/6; ANOVA with Dunnett's post hoc test with *APPPS1* as control group, ns.

(plaque formation), and 8 months (full plaque pathology and cognitive deficits) and compared to age-matched wild-type, *Becn1*$^{+/-}$ and *APPPS1* mice. The brains were processed in different buffers, resulting in four fractions containing proteins with different solubility (Kawarabayashi *et al*, 2001). The content of pro-inflammatory cytokines in the fractions containing highly soluble proteins (TBS and TX fraction) was analyzed by electrochemiluminescence (Meso Scale). While 3-month-old mice showed similar levels of IL-1beta regardless of the genotype, brain lysates of 4- and 8-month-old *APPPS1 Becn1*$^{+/-}$ mice contained significantly more IL-1beta in both fractions (Fig 2E). In contrast, TNFalpha was not altered at all and IL-6 was only increased in the TX fraction but not the TBS fraction of 8-month-old *APPPS1 Becn1*$^{+/-}$ mice (Fig EV1D and E).

To determine whether an increase in IL-1beta expression in *APPPS1 Becn1*$^{+/-}$ mice may affect amyloid-beta pathology, we quantified the amount of amyloid-beta 1–40 and amyloid-beta 1–42 in protein lysates of brains from age-matched *APPPS1* and *APPPS1 Becn1*$^{+/-}$ 3-, 4-, and 8-month-old mice by means of Meso Scale (Fig 2F) as well as by morphometric analyses of immunostained histological sections from brains of 4-month-old mice (Fig EV2A–C). Since we were not able to detect a significant difference in amyloid burden as well as in plaque size and plaque distribution in *APPPS1* versus *APPPS1 Becn1*$^{+/-}$ mice (Figs 2F and EV2A–C), we compared the phagocytic capacity of microglia in acute brain slices from 4-month-old *Becn1*$^{+/-}$ mice to those of microglia from wild-type mice. Again, no significant differences with respect to the amount of phagocytic cells or the overall phagocytic index became apparent (Fig EV2D–F). Taken together, these data demonstrate that reducing BECN1 and, thus, a diminution in autophagy increased specifically the release of IL-1beta and IL-18 from acute activated (LPS/ATP) and primed (amyloid-beta) microglia *in vitro* and *in vivo*, but did not substantially alter amyloid-beta pathology or phagocytosis *in vivo*.

Reduction in BECN1 influences the IL-1beta and IL-18 processing pathway

In order to assess the mechanism by which BECN1 is influencing IL-1beta and IL-18 production and/or release, we investigated the crucial steps in the common pathway of IL-1beta and IL-18 production. The pro-inflammatory response starts with transcription and translation of the IL-1beta and IL-18 precursors followed by their processing at the inflammasome (Walsh *et al*, 2014). Therefore, microglia isolated from newborn *Becn1*$^{+/-}$ and wild-type mouse pups were stimulated with LPS and ATP and the levels of pro-IL-1beta protein were determined by Western blotting. No differences in the levels of pro-IL-1beta were discernible (Fig EV3A).

Subsequently, the formation and assembly of the inflammasome, the protein complex responsible for processing pro-IL-1beta to IL-1beta by CASP1, were analyzed. The protein levels of NLRP3, the sensor component of the inflammasome, were analyzed by Western blotting in *Becn1*$^{+/-}$ and wild-type microglia. While non treated cells expressed only low levels of NLRP3, stimulation with LPS/ATP increased NLRP3 expression strongly and activated microglia of *Becn1*$^{+/-}$ mice contained significantly more NLRP3 than microglia of wild-type mice (Fig 3A). In contrast, no difference between the *Nlrp3* mRNA levels of *Becn1*$^{+/-}$ and wild-type microglia was apparent (Fig 3B).

Next, inflammasome assembly was investigated by staining of ASC (apoptosis-associated speck-like protein containing a carboxy-terminal CARD), the adaptor protein for pro-CASP1 binding and processing. Again, microglia isolated from newborn *Becn1*$^{+/-}$ and wild-type mouse pups were stimulated with LPS and ATP or left untreated. In non treated cells, ASC showed diffuse staining in the cytoplasm (Fig 3C). However, after stimulation, formation of inflammasomes could be observed in a subpopulation of cells, as well as release of inflammasomes after pyroptosis/ejection (Baroja-Mazo *et al*, 2014; Franklin *et al*, 2014). Quantification of these ASC foci in stimulated cells showed an almost threefold increased presence of inflammasomes in or around *Becn1*$^{+/-}$ microglia (Fig 3C).

Finally, pro-CASP1 as substrate for the inflammasome and the processed, active CASP1 was analyzed. Pro-CASP1 protein levels in cell lysates of LPS/ATP-stimulated microglia showed no difference between *Becn1*$^{+/-}$ and wild-type cells (Fig EV3B). However, Western blotting of the cell supernatant from stimulated microglia revealed that a significantly higher amount of cleaved, active CASP1 p10 was released from *Becn1*$^{+/-}$ microglia compared to wild-type

 © 2019 The Authors

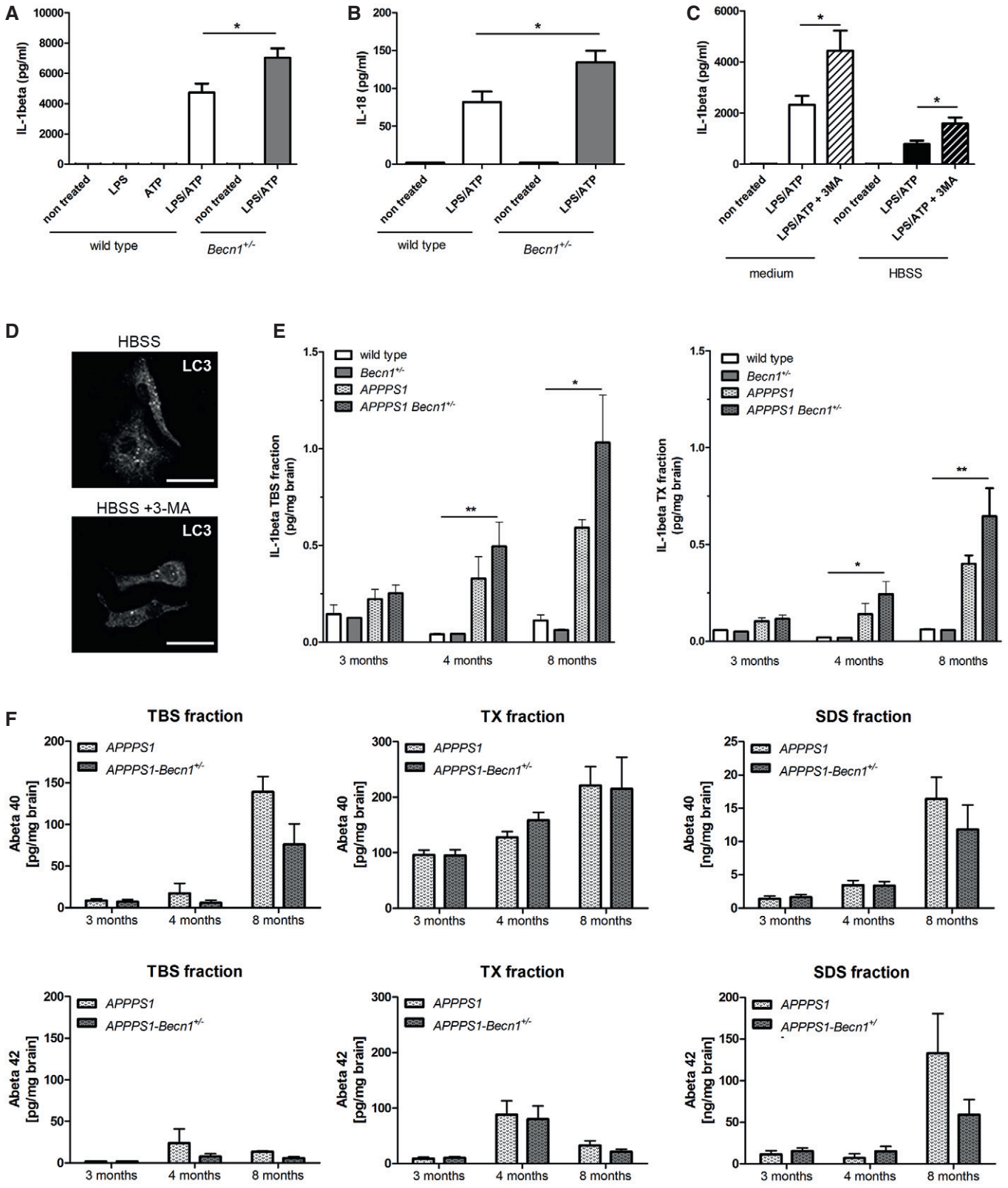

Figure 2.

microglia (Fig 3D). In addition, 3-MA treatment of wild-type microglia significantly increased the CASP1 p10 levels in the cell supernatant (Fig EV3C).

Taken together, these data indicate that the increase in IL-1beta and IL-18 production in *Becn1*$^{+/-}$ microglia is linked to an upregulation of inflammasome formation and/or slower turnover.

© 2019 The Authors

NLRP3 is a substrate for autophagy

To determine the molecular mechanism of the effects described above, we assessed in detail how reduced BECN1 could mediate the observed increase in NLRP3 and inflammasomes in *Becn1*$^{+/-}$ microglia. To obtain a comprehensive impression of NLRP3 appearance, and spatial distribution, endogenous NLRP3 was analyzed by immunocytochemistry. Non treated microglia showed, in correlation to their weak band in the Western blot, a diffuse cytoplasmic staining with a few small NLRP3 puncta (Fig 4A). Stimulation of microglia with LPS/ATP resulted in the emergence of more and larger NLRP3 puncta/specs of different sizes (Fig 4A, arrows), indicating formation of NLRP3 oligomers or aggregates (Susjan *et al*, 2017) (see also Discussion). Quantification of NLRP3 aggregates in *Becn1*$^{+/-}$ and wild-type microglia showed a higher number of NLRP3 aggregates in *Becn1*$^{+/-}$ microglia (Fig EV4A). These data are in agreement with the NLRP3 protein levels quantified by Western blotting (Fig 3A). The subcellular localization as

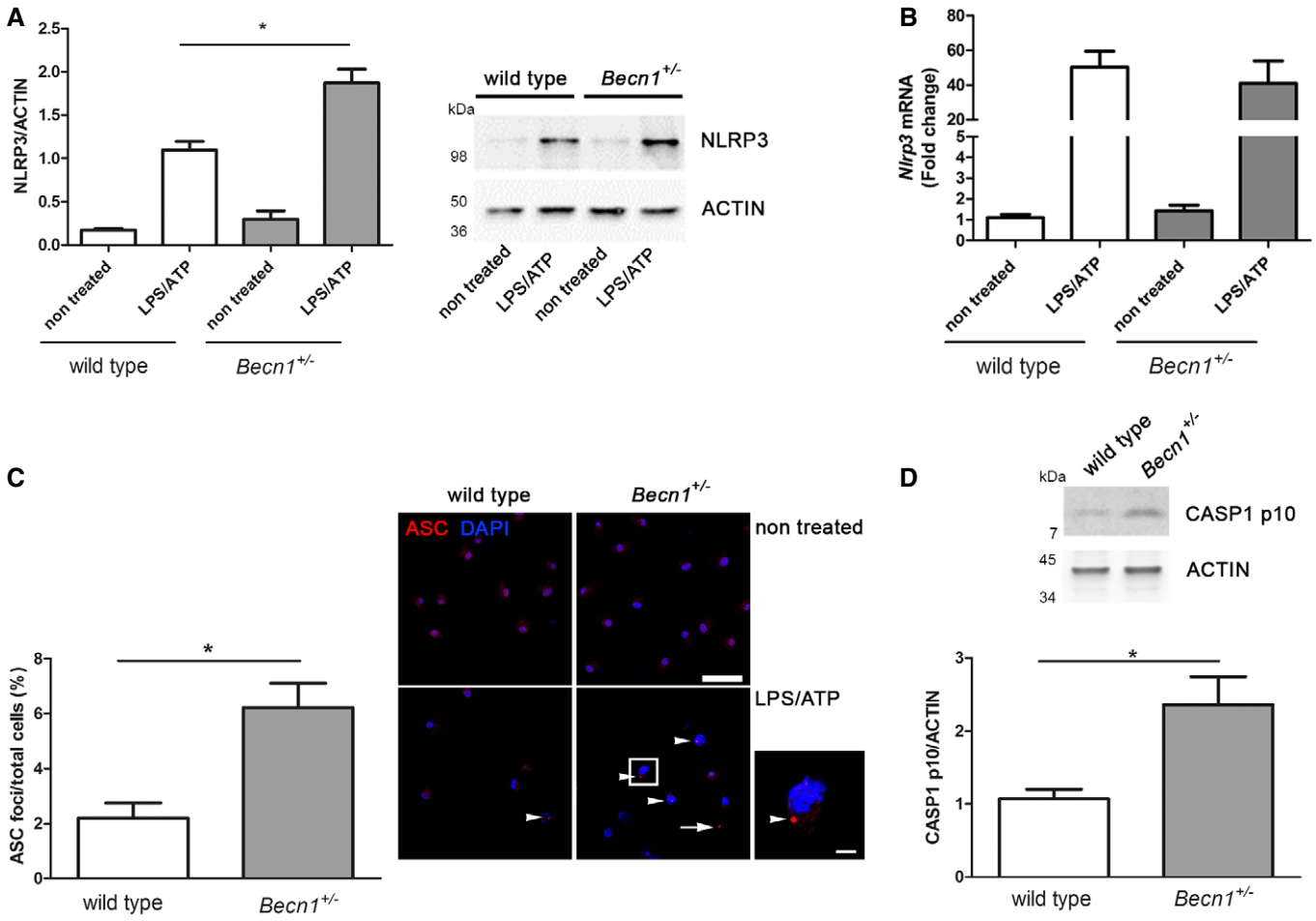

Figure 3. Reduction in BECN1 influences the IL-1beta processing pathway.

A The expression of NLRP3 protein in non treated and LPS/ATP-treated wild-type and *Becn1*$^{+/-}$ microglia was determined by Western blot and normalized to ACTIN. Reduction in BECN1 significantly enhanced expression of NLRP3; mean ± SEM, wild-type $n = 4$, wild-type LPS/ATP $n = 9$, *Becn1*$^{+/-}$ $n = 4$, *Becn1*$^{+/-}$ LPS/ATP $n = 23$; ANOVA with Tukey's post hoc test $^*P < 0.05$.

B The expression of *Nlrp3* mRNA in non treated and LPS/ATP-treated wild-type and *Becn1*$^{+/-}$ microglia was determined by qPCR. No significant differences can be detected between wild-type and *Becn1*$^{+/-}$ microglia; mean ± SEM, wild-type: $n = 7$, *Becn1*$^{+/-}$: $n = 3$; ANOVA with Tukey's post hoc test, ns for LPS/ATP-treated wild-type versus *Becn1*$^{+/-}$.

C LPS/ATP-treated and non treated wild-type and *Becn1*$^{+/-}$ microglia were immunolabeled for ASC (red) and imaged by confocal microscopy to investigate the assembly of inflammasomes. In non-stimulated cells, ASC is distributed diffusely in the cytoplasm (upper panels). However, after stimulation, formation of inflammasomes (arrowheads) can be detected in a subpopulation of cells as well as release of inflammasomes after pyroptosis/ejection (arrow). Quantification showed a significantly increased percentage of inflammasomes in or around *Becn1*$^{+/-}$ microglia; mean ± SEM, wild-type LPS/ATP $n = 4$, *Becn1*$^{+/-}$ LPS/ATP $n = 7$; two-tailed *t*-test $^*P < 0.05$; scale bar: 50 μm, insert scale bar: 10 μm.

D The presence of cleaved CASP1 (p10) protein in the supernatant of LPS/ATP-treated wild-type and *Becn1*$^{+/-}$ microglia was determined by Western blot and normalized to ACTIN. Reduction in BECN1 significantly enhanced release of CASP1; mean ± SEM, wild-type LPS/ATP $n = 8$, *Becn1*$^{+/-}$ LPS/ATP $n = 18$; two-tailed *t*-test $^*P < 0.05$.

Source data are available online for this figure.

© 2019 The Authors

Figure 4. NLRP3 and LC3-positive vesicles are closely associated.

A LPS/ATP-treated and non treated wild-type and *Becn1*$^{+/-}$ microglia were immunolabeled for NLRP3 (green) and LC3 (red) and imaged by confocal microscopy. Stimulation resulted in the appearance of many NLRP3-containing aggregates of different sizes (arrows). In non treated cells, only a few overlapping signals with LC3-stained autophagosomes (arrowheads) are visible. Stimulated microglia, however, showed multiple colocalizations of LC3-positive vesicles and NLRP3 aggregates; scale bar: 7.5 μm.

B LPS/ATP-treated wild-type microglia were immunolabeled for NLRP3 (green) and LC3 (red) and analyzed by super-resolation microscopy (SIM). NLRP3 aggregates of different sizes coclustering with LC3-positive autophagosomes are clearly visible. 3D volume rendering of large (I) and small (II) NLRP3 aggregates from the magnified ROIs showed engulfment of NLRP3 by autophagosomes; scale bar: 10 μm; magnified ROIs: 1 μm.

C 3D radial intensity profiles of NLRP3 and LC3 signals derived from SIM images in wild-type microglia, centered on the maxima of NLRP3 clusters. The radial profiles confirm that both proteins colocalize to the same organelle; mean ± SEM, n = 4.

determined by the 3-dimensional distance of NLRP3 aggregates to the nucleus did not differ between *Becn1*$^{+/-}$ and wild-type microglia (Fig EV4B). To confirm the specificity of the NLRP3 staining, stimulated microglia were co-labeled with ASC. As described previously (Walsh *et al*, 2014), we observed a very close association and partial overlap of NLRP3 and ASC signals using confocal and super-resolution microscopy (Fig EV4C and D).

To investigate the fate of the NLRP3 puncta/aggregates, microglia from *Becn1*$^{+/-}$ and wild-type mouse pups were treated with LPS and ATP (alongside non treated controls) and then stained for endogenous NLRP3 and LC3. Confocal microscopy of non treated cells showed only a few overlapping signals of LC3-stained vesicles (arrowheads) and small NLRP3 puncta (arrows) (Fig 4A). However, stimulated microglia contained many LC3-positive vesicles that strongly colocalized with NLRP3 aggregates of different sizes (Fig 4A). These colocalizations appeared in both *Becn1*$^{+/-}$ and wild-type microglia, indicating engulfment and probable degradation of NLRP3 by autophagosomes. As NLRP3 has been shown to colocalize with mitochondria (Zhou *et al*, 2011; Subramanian *et al*, 2013; Bracey *et al*, 2014), the localization of MTR-stained mitochondria, NLRP3, and LC3 was determined by confocal microscopy of LPS/ATP-stimulated cells. NLRP3 was found to colocalize not only with LC3, but also with MTR-stained mitochondria, and NLRP3 aggregates/puncta were in addition detectable in close vicinity to mitochondria though not directly colocalizing. A colocalization of NLRP3, LC3, and mitochondria was, however, not observed (Fig EV4E).

To gain a deeper understanding of the interaction of NLRP3 and autophagosomes, we performed 3D structured illumination microscopy (SIM), a super-resolution microscopy method that increases the conventional spatial resolution (i.e., confocal) by factor 2 in all three dimensions. SIM and subsequent 3D volume rendering of large (I) and small (II) NLRP3 aggregates showed indeed that LC3-positive structures corral around and partially overlap with the NLRP3 clusters in wild-type (Fig 4B) and *Becn1*$^{+/-}$ microglia (Appendix Fig S1A, see also Appendix videos of 3D projections). In order to confirm that NLRP3 clusters really present a substrate for autophagy, we quantified the colocalization of NLRP3 and LC3 by performing 3D radial intensity profiles around the center of NLRP3 clusters (Figs 4C and 5D). Indeed, both proteins colocalized to the same organelle as indicated by an overlap of both maxima in the radial intensity profile. The signal decay within the known size of autophagosomes (Mizushima *et al*, 2002) indicates that NLRP3 aggregates were indeed engulfed/taken up by the LC3-positive vesicles (Fig 4C, Appendix Fig S1B and C).

To assess whether NLRP3 aggregates exist also in microglia of adult mice, an *ex vivo* approach was employed: Microglia were isolated from 8-month-old wild-type and *APPPS1* mice and cultivated for 4 h. Subsequent confocal microscopy revealed NLRP3 aggregates as well as LC3-positive vesicles inside these cells. Furthermore, some NLRP3 signals colocalized with LC3, further supporting the conclusion that NLRP3 degradation occurs through autophagy (Fig EV5A). In contrast to microglia, neonatal murine astrocytes as yet another cytokine-producing brain cell did not contain NLRP3 (Fig EV5B and C).

CALCOCO2/NDP52 colocalizes with NLRP3 and modulates IL-1beta release

In order to determine the interaction between NLRP3 and the vesicles on the molecular level, we investigated possible adaptor proteins. p62/SQSTM1 has been described as an adaptor protein for the autophagic removal of inflammasomes (Shi *et al*, 2012). Therefore, we stained NLRP3 and p62 in LPS/ATP-treated but detected no colocalization (Appendix Fig S2A). In contrast, CALCOCO2/NDP52 (arrowheads) which acts as an autophagic adaptor protein in human cells colocalized with smaller and larger NLRP3 aggregates (arrows) in LPS/ATP stimulated wild-type microglia (Fig 5A). SIM confirmed that both proteins were in very close proximity (Fig 5B); the same could also be shown for LPS/ATP-treated *Becn1*$^{+/-}$ microglia (Appendix Fig S2B). The colocalization of NLRP3 and CALCOCO2 was confirmed by performing 3D radial intensity profiles on NLRP3 clusters in wild-type (Fig 5C) and *Becn1*$^{+/-}$ microglia (Appendix Fig S2C). To further substantiate this interaction and to investigate the location of both proteins within the autophagosome, we used the SIM images from wild-type microglia and compared the LC3 and CALCOCO2 signal in the center of NLRP3 clusters with its maximal intensity within the cluster. Clearly, the relative center intensity of CALCOCO2 (~95%) was significantly higher than the center intensity of LC3 (~60%) (Fig 5D). These data strongly suggest that NLRP3 interacts with CALCOCO2 within the lumen of autophagosomes, while LC3 is localized to both sides of the autophagosomal membrane.

Murine cells express a truncated form of CALCOCO2 containing the SKICH, LIR, and coiled-coil domain but not the ubiquitin-binding and galectin-8 domains (Tumbarello *et al*, 2015). To determine whether the close localization of murine CALCOCO2 to NLRP3 may have a functional impact and is related to cytokine production, microglia were treated with a CALCOCO2 siRNA, which resulted in significant reduction in the protein (Fig 5E). After LPS/ATP stimulation, cells with CALCOCO2 knockdown released more IL-1beta into the supernatant (Fig 5F), while TNFalpha and IL-6 levels remained unchanged (Fig EV5D and E) compared to microglia transfected with a scrambled siRNA. These data support the idea that CALCOCO2 binds NLRP3 most probably via the SKICH domain (see Discussion) and is involved in the modulation of IL-1beta response.

© 2019 The Authors

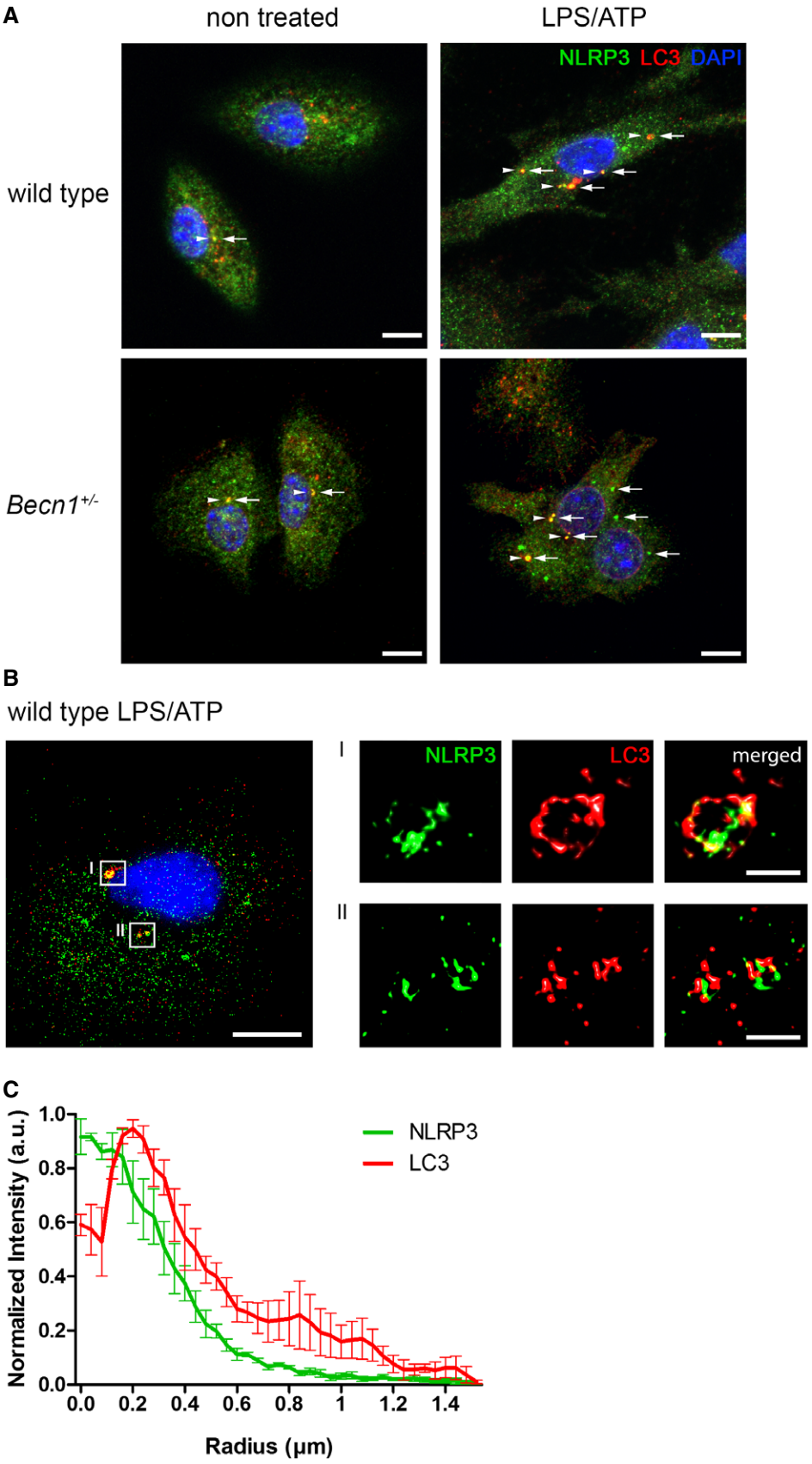

Figure 4.

© 2019 The Authors

Figure 5. CALCOCO2/NDP52 colocalizes with NLRP3 and modulates IL-1beta release.

A LPS/ATP-treated wild-type microglia were stained for NLRP3 (green) and CALCOCO2 (red) and analyzed by confocal microscopy. Colocalizations of NLRP3 aggregates (arrows) and CALCOCO2 (arrowheads) are apparent; scale bar: 10 μm.

B LPS/ATP-treated wild-type microglia were stained for NLRP3 (green) and CALCOCO2 (red) and analyzed by super-resolation microscopy (SIM). NLRP3 aggregates coclustering with CALCOCO2-positive signals are visible. 3D volume rendering of NLRP3 aggregates from the magnified ROIs showed close contact of NLRP3 with CALCOCO2; scale bar: 10 μm; magnified ROIs: 1 μm.

C 3D Radial intensity profiles of NLRP3 and CALCOCO2 signals derived from SIM images in wild-type microglia, centered on the maxima of NLRP3 clusters. The radial profiles confirm that both proteins colocalize; mean ± SEM, $n = 3$.

D In SIM images from wild-type microglia the subautophagosomal localization of LC3 and CALCOCO2 was analyzed in relation to NLRP3. LC3 and CALCOCO2 intensities at the center of NLRP3 aggregates were normalized to their maximum within the same cluster. While CALCOCO2 intensity is near maximal at the center of NLRP3 aggregates (indicating the lumenal localization of CALCOCO2), the relative LC3 intensity was significantly lower (in agreement with the LC3 localization at autophagosomal membranes); LC3: $n = 4$, CALCOCO2: $n = 3$; two-tailed t-test $^{**}P < 0.01$.

E Microglia from *Becn1*$^{+/-}$ mice were transfected with scrambled siRNA or with siRNA for CALCOCO2. 6 d after transfection, cells were stimulated with LPS/ATP. The expression of CALCOCO2 protein was determined by Western blot. Application of CALCOCO2 siRNA resulted in significantly reduced expression of CALCOCO2; mean ± SEM, $n = 3$; two-tailed t-test $^{*}P < 0.05$.

F The amount of IL-1beta in the supernatant released from the cells described in (E) was determined by ELISA. Microglia with a CALCOCO2 knockdown released significantly more IL-1beta; mean ± SEM, $n = 3$; two-tailed t-test $^{*}P < 0.05$.

Discussion

In this study, we analyzed the effects of reduced BECN1 levels on the inflammatory process in microglia *in vitro* after an acute pro-inflammatory stimulus and *in vivo* in an AD-like mouse model with amyloid-beta pathology and neuroinflammation. Impaired autophagy has been linked to AD in various ways as detailed in recent reviews (Menzies *et al*, 2015, 2017), but research until now has concentrated almost exclusively on neurons. However, neuroinflammation is an important driver of AD (Heppner *et al*, 2015), and since microglia are the main producers of pro-inflammatory cytokines in the brain, they are in the center of interest when investigating neuroinflammation. BECN1 is a key protein of the autophagic pathway, and its reduction in *Becn1*$^{+/-}$ mice resulted accordingly in diminished autophagic flux and autophagosome formation. This is in agreement with reports demonstrating reduced autophagy in neurons, muscle, and endothelial cells isolated from *Becn1*$^{+/-}$ mice (Qu *et al*, 2003; Pickford *et al*, 2008), which further indicates that microglial BECN1 reduction impairs autophagy. *Becn1*$^{-/-}$ microglia could not be employed in this study since *Becn1*$^{-/-}$ embryos die *in utero* very early between E7.5 and E8.5 (Yue *et al*, 2003), thus at a time point before microglia precursors leave the yolk sac to colonize the developing brain (starting at E9.5) (Ginhoux *et al*, 2010; Swinnen *et al*, 2013; Tay *et al*, 2017).

In vitro genetic reduction in *Becn1* or addition of the autophagy blocker 3-MA resulted in increased expression of IL-1beta and IL-18 after addition of a standard acute pro-inflammatory stimulus (LPS followed by ATP), while TNFalpha or IL-6 was not altered. The specific targeting of the IL-1beta/IL-18 pathway by impaired autophagy is in agreement with previous data showing no effect on TNFalpha release after knockdown of *Atg7* in neonatal microglia (Cho *et al*, 2014). In contrast, Ye *et al* (2017) observed not only enhanced IL-1beta levels, but also an increase in TNFalpha and IL-6 after impairment of autophagy by 3-MA, or after knockdown of *Becn1* or *Atg5* in the microglial cell line BV2. Additionally, Santeford *et al* (2016) also described enhanced IL-6 levels after loss of *Atg5*. A recent analysis of microglia from different origins revealed that the expression profile of primary microglia differs from BV2 cells, where neonatal primary microglia resemble adult microglia more closely than BV2 cells, which could account for the different findings (Butovsky *et al*, 2014). Also, macrophages with loss of *Atg16l1* exhibited a specific increase in IL-1beta/IL-18 production and showed no effect on TNFalpha or IL-6 production (Saitoh *et al*, 2008). Based on these data, we conclude that the observed increase in IL-1beta/IL-18 production in *Becn1*$^{+/-}$ microglia is not caused by a general microglial priming and activation mediated by impaired autophagy, but rather a specific intervention of the IL-1beta/IL-18 processing pathway.

To support this hypothesis, we analyzed whether reduction in BECN1 also increased IL-1beta levels *in vivo* in an Alzheimer-like setting using the established amyloid pathology model *APPPS1* (Radde *et al*, 2006). Production of IL-1beta in microglia occurs *in vivo* only after priming (Perry & Holmes, 2014) and the *Il1b* gene is upregulated in primed microglia of *APPPS1* mice, as well as in acutely LPS-activated microglia as shown in a differential transcriptome analysis (Holtman *et al*, 2015). Heterozygous loss of *Becn1* alone did not result in increased IL-1beta protein levels in the brain compared to age-matched wild-type mice. As the oldest analyzed mice were only 8 months old, an aging-mediated effect had apparently not yet occurred. However, it could be possible that older mice show an impact of *Becn1* heterozygosity, as 24-month-old mice exhibited an upregulation of *Il1b* (Holtman *et al*, 2015).

In support of this hypothesis, we observed a significant age-dependent upregulation of IL-1beta in TBS and TX protein fractions from the brains from 4- and 8-month-old *APPPS1 Becn1*$^{+/-}$ mice. Thus, when microglia were primed by extracellular amyloid-beta, the reduced levels of BECN1 mediated an increase in IL-1beta production. *In vitro*, this was an IL-1beta specific effect, as no changes in TNFalpha were observed. However, the impact of BECN1 reduction on IL-6 remains unclear. While no effect on IL-6 release was observed *in vitro* and *in vivo* in the TBS fraction, an increase in IL-6 in the TX fraction of 8-month-old *APPPS1 Becn1*$^{+/-}$ mice became apparent, warranting further investigation.

In *APPPS1 Becn1*$^{+/-}$ mice, neither changes in the amyloid-beta load were detected nor phagocytosis was altered. On first sight, this appears to be in contrast to data from Pickford *et al* (2008), who observed an increase in amyloid pathology in 9-month-old *T41APP Becn1*$^{+/-}$ mice. However, this difference can be explained by the fact that another transgenic mouse strains were used in our experiments, particularly by the strong impact of the two overexpressed transgenes *APP* and *PS1* in *APPPS1* mice used herein. Knockdown of *Becn1* in BV2 microglial cells has been shown to reduce

© 2019 The Authors

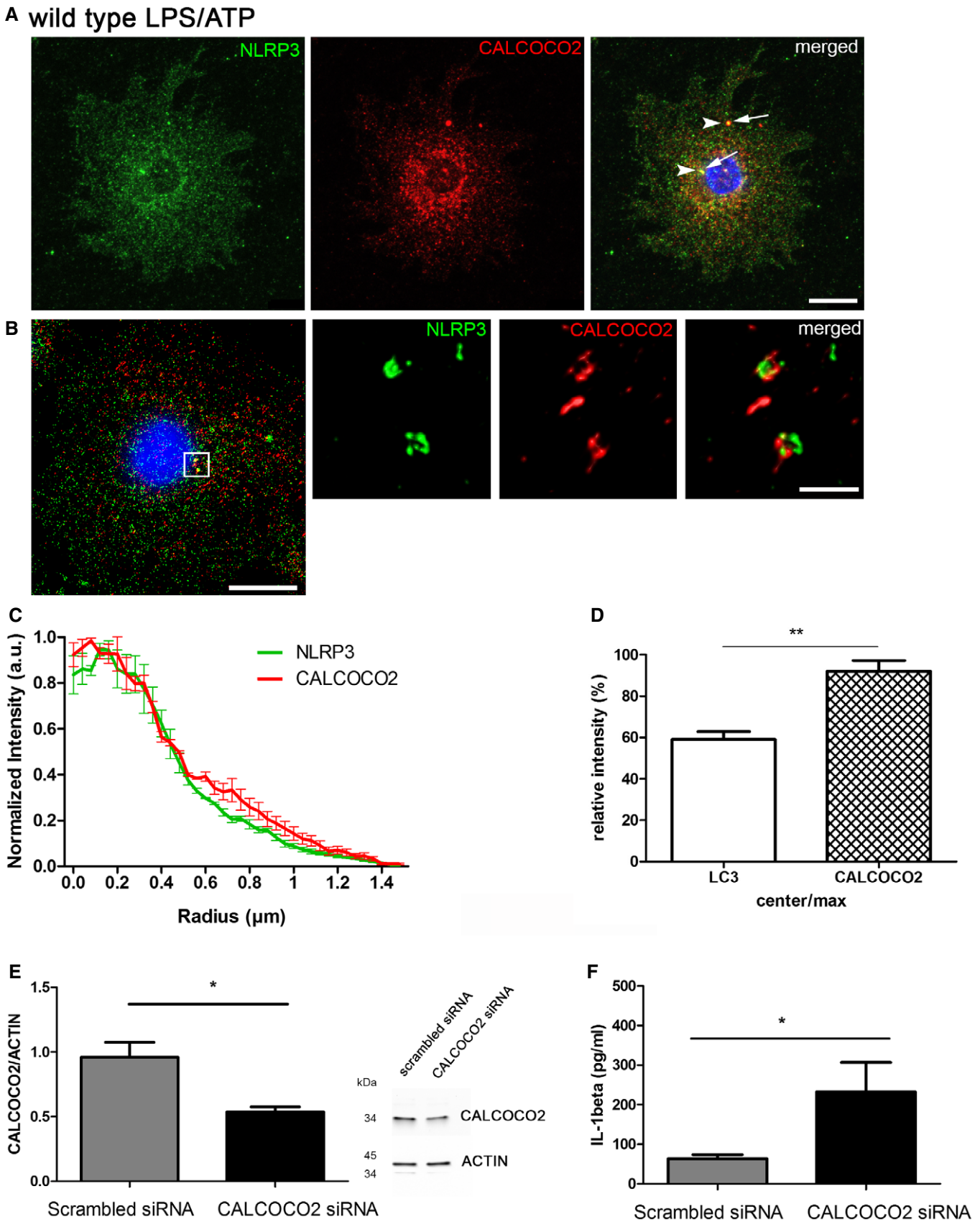

Figure 5.

© 2019 The Authors

phagocytosis (Lucin *et al*, 2013), while an increase in IL-1beta expression is supposed to augment the phagocytic activity (Ferreira *et al*, 2011). While the lack of a difference in phagocytosis in *APPPS1 Becn1*$^{+/-}$ microglia certainly explains why there is no substantial difference in amyloid-beta burden in *APPPS1* mice with one versus two alleles of *Becn1*, it appeared to be counter-intuitive at first sight, also in light of previous data showing that IL-1beta release can drive the phagocytic capacity of microglia. However and importantly, Lucin *et al* (2013) demonstrated that knocking down Beclin1 in BV2 microglial cells reduces the phagocytic capacity of these cells. Based on this, we assume that the Beclin1-mediated decrease in phagocytosis, which should also apply to *Becn1*$^{+/-}$ microglia, may be compensated by the IL-1beta-driven reverse effect, that is, that in heterozygous *Becn1*$^{+/-}$ microglia these opposing effects modulating phagocytosis outcompete each other. Along this line, one would speculate that *APPPS1* mice with a homozygous deletion of Beclin1 are expected to harbor microglia with reduced phagocytic microglia, supposedly resulting in an increase in amyloid pathology. The respective experimental *in vivo* proof of this hypothesis is, however, difficult to provide given that homozygous Beclin1 knock-out mice are lethal (Qu *et al*, 2003; Yue *et al*, 2003). Future studies, perhaps with older mice, may answer this question. Alternatively, a microglia-targeted complete loss of BECN1 by using a *Becn1*$^{flox/flox}$ mouse crossed to a *Cx3cr1*^{Cre} or *Sall1*^{Cre} mouse could maximize the effects shown here.

A fundamental question is the mechanism by which reduced BECN1 levels and autophagy modulate the IL-1beta/IL-18 production. Proposed mechanisms include degradation of pro-IL-1beta (Harris *et al*, 2011), degradation of inflammasomes (Shi *et al*, 2012), and an indirect activation of the inflammasome via accumulation of dysfunctional mitochondria and oxidative stress due to impaired mitophagy (Saitoh *et al*, 2008; Zhou *et al*, 2011; Lodder *et al*, 2015; Lee *et al*, 2016; Ye *et al*, 2017). Since no significant changes in pro-IL-1beta levels were observed, we investigated other steps in the IL-1beta/IL-18 processing pathway. Here, increased levels of NLRP3 and cleaved CASP1 alongside a higher percentage of cells with ASC-stained inflammasomes were detected. Pro-CASP1 is cleaved into p10 and p20 fragments, which were reported to be degraded via the ubiquitin–proteasome system (Squires *et al*, 2007; Muehlbauer *et al*, 2010; Van Opdenbosch *et al*, 2014). Therefore, SIM was used as a super-resolation microscopy method to determine the fate of NLRP3 and the inflammasomes. Staining of endogenous NLRP3 in LPS/ATP-stimulated microglia revealed several distinct, highly fluorescent NLRP3 puncta/specs in addition to a rather diffuse cytoplasmic staining, which was also observed in non treated cells. The specificity of the NLRP3 staining was confirmed using SIM by co-staining with ASC: An intimate contact between NLRP3 and ASC in activated cells could be observed. Structurally, this interaction resembled the NLRP3-ASC interaction observed in the *Salmonella*-induced inflammasome (Man *et al*, 2014), where ASC is forming a ring-like scaffold for NLRP3. One apparent difference is the presence of two or more intervened ASC rings in the inflammasome of LSP/ATP-stimulated microglia, which is not seen in *Salmonella*-induced inflammasome activation.

The co-staining of endogenous LC3 and NLRP3 revealed numerous colocalizations of both signals. This correlates with data of Chuang *et al* (2013) that showed colocalization of overexpressed and fluorescence-tagged LC3 and NLRP3 in HEK293 cells. Stimulated myeloid cells normally contain only one or two ASC-containing inflammasomes (Baroja-Mazo *et al*, 2014; Franklin *et al*, 2014) (see also Fig 3C) that are also significantly larger than most of the NLRP3 signals seen in these cells (see Fig EV4C and D). Murine NLRP3 has a calculated molecular weight of 113 kDa and the pyrin domain has to exist at least as a trimer to trigger IL-1beta production, which is apparently independent of the formation of ASC-containing inflammasome (Susjan *et al*, 2017). Thus, it seems plausible that the observed smaller NLRP3 aggregates present NLRP3 trimers or higher oligomeric forms as suggested for NLRP2 (Faustin *et al*, 2007) or NLRC4 (Hu *et al*, 2015; Zhang *et al*, 2015). The large NLRP3-positive aggregates are likely part of a completely assembled, ASC-containing inflammasome. NLRP3 colocalized with mitochondria as shown before (Zhou *et al*, 2011; Subramanian *et al*, 2013; Bracey *et al*, 2014), whereas we could not observe a colocalization of NLRP3, mitochondria, and LC3, indicating that mitochondria are not involved in the degradation of NLRP3, or that NLRP3 has no substantial impact on mitophagy, respectively.

SIM pictures of small and large NLRP3 aggregates confirmed the localization of NLRP3 to LC3-positive autophagosomes. The described adaptor protein for the autophagic removal of inflammasomes, p62/SQSTM1 (Shi *et al*, 2012), did not colocalize with or bind to NLRP3. In contrast, CALCOCO2 interacted directly with NLRP3 and was located significantly nearer to NLRP3 than LC3 in the SIM images. CALCOCO2 has been shown to be involved in mitophagy (Moore & Holzbaur, 2016) and xenophagy (Verlhac *et al*, 2015) in human cells. Murine cells express only a truncated version of CALCOCO2 and its functionality is under discussion. However, the murine protein still contains the SKICH and LIR domain and several domain-specific knock-out studies in CALCOCO2 showed that the SKICH domain is essential for binding TRIF, TRAF6 (Inomata *et al*, 2012), phosphorylated tau, amyloid-beta (Jo *et al*, 2014), and damaged mitochondria (Furuya *et al*, 2018). The LIR domain specifically binds LC3C on the autophagosomal membrane, which then attracts all other ATG8 orthologues (von Muhlinen *et al*, 2013). Our data show that CALCOCO2 is located between NLRP3 and LC3 in a vesicle resembling the size of an autophagosome. While it appears that murine CALCOCO2 is able to bind NLRP3 via its SKICH domain, it is not yet entirely solved whether it acts as an autophagic adaptor protein by also binding LC3, or whether additional proteins are involved in the degradation process to compensate for the missing ubiquitin-binding domain. However, the downregulation of CALCOCO2 by siRNA in microglia resulted in an increase in IL-1beta expression, while TNFalpha and IL-6 were not affected, implying that murine CALCOCO2, despite its truncation, is involved in regulating IL-1beta production in murine microglia.

Materials and Methods

Mice

APPPS1$^{+/-}$ mice were described before (Radde *et al*, 2006). Male *APPPS1*$^{+/-}$ mice were crossed to female Bl6J mice, and *APPPS1*$^{+/-}$ mice were compared to littermate wild-type controls. *Becn1*$^{+/-}$ mice have also been described before (Qu *et al*, 2003) and were a gift from Tony Wyss-Coray (Stanford University School of Medicine/USA). Mice were bred from heterozygous matings. *Becn1*$^{+/-}$ mice

© 2019 The Authors

were compared to littermate wild-type controls. Animals were kept in individually ventilated cages with a 12-h light cycle with food and water *ad libitum*. All animal experiments were conducted in accordance with animal welfare acts and were approved by the regional office for health and social service in Berlin (LaGeSo).

Microglia isolation and culture

Newborn animals (2–4 days) were killed by decapitation. The meninges were removed, and the brain was homogenized. Cells were separated by incubation with 0.1% trypsin for 15 min at 37°C. Cells were cultivated at 37°C with 5% CO_2 and 95% air in DMEM (41966-029, Invitrogen) with 10% FCS (Invitrogen) and 1% penicillin/streptomycin (Invitrogen) for 7 DIV until a confluent glial cell layer (astrocytes and microglia) was formed. To induce microglial proliferation, the mixed glial culture was stimulated from day 7 on with GM-CSF (Miltenyi Biotec, 130-095-746) with a final concentration of 5 ng/ml. Microglia were harvested at DIV 10–14 by 6 min of shaking. Microglial identity was confirmed by immunostaining for Iba1 and CD68.

Adult animals were anesthetized with isoflurane, euthanized by CO2, and transcardially perfused with 1× PBS. The brain was removed and dissected, followed by homogenizing using the gentle MACS Octo Dissociator (Miltenyi Biotec). Next, magnetic sorting using CD11b+ magnetic beads (Miltenyi Biotec, 130-093-634) was performed. Prior to (i.e., directly after tissue dissociation) and after MACS sorting, isolated cells are stained with CD45 and CD11b antibodies and analyzed by flow cytometry using the expression levels of CD11b and of CD45 to distinguish resident microglia (CD11b+CD45int) from other CNS macrophages (CD11b+CD45hi) including meningeal macrophages or from other (systemic) inflammatory cells such as peripheral leukocytes (CD11b-CD45hi). Only isolations with a purity of 95% of CD11b-positive macrophages/microglia were used for further analysis.

After sorting, the cells were seeded on PLL-coated coverslips, 1×10^6 cells/well, and fixed with ice-cold methanol after 3 h at 37°C. Subsequently, they were stained for LC3 and NLRP3, see Immunocytochemistry section.

Microglia treatment

Microglia from newborn mice were seeded in 24-well plates and incubated overnight in growth medium DMEM (Invitrogen) with 10% FCS (Invitrogen) and 1% penicillin/streptomycin (Invitrogen) without GM-CSF. Next day, cells were kept for 2 h in growth medium or HBSS as indicated. As a pro-inflammatory stimulus, LPS (final concentration 1 μg/ml) for 3 h followed by ATP (final concentration 1 mM) for 45 min was used before supernatant and cells were harvested. 3-MA (Sigma-Aldrich, M9282, final concentration 10 mM) was added 1 h 45 min before the end of the experiment. To measure autophagic flux, microglia were kept for 2 h in cultivation medium or HBSS (24020-091, Invitrogen) in the presence of Bafilomycin A1 (Sigma-Aldrich, B1793, final concentration 5 nM).

siRNA transfection

Microglia were seeded as described above. Next day, medium was exchanged and cells were transfected with a complex of Viromer Blue (Lipocalyx, VB-01LB-00) and CALCOCO2 FlexiTube siRNA #4 (Qiagen, 1027416/GS76815), according to manufacturer's instruction. Every 2 days, fresh medium was added to the wells. Six days after transfection, cells were stimulated with LPS/ATP as described above.

ELISA

The supernatant of stimulated microglia was diluted 1:10-1:20 or used undiluted (IL-18). IL-1beta (eBioscience, 88701388), IL-18 (MBL, MBL-7625), TNFalpha (eBioscience, 88723477), and IL-6 (eBioscience, 88706488) concentration was determined according to the manufacturer's instructions.

The cytokine content as well as the amyloid-beta burden of the whole brain was determined using a MESO QuickPlex SQ 120 system (Meso Scale Discovery) and the V-PLEX Pro-inflammatory Panel 1 (Meso Scale Discovery, K15048D1) and the V-PLEX Aβ Peptide Panel 1 (4G8) (Meso Scale Discovery, K15199E), respectively. Proteins were extracted from mouse brains using the four-step protocol as described before (Kawarabayashi *et al*, 2001). The TBS fraction and the Triton-X fraction containing the soluble proteins were measured without further dilution. The SDS fraction was diluted 1:500 prior to measuring insoluble proteins.

Western blotting

Protein lysates were separated by SDS–PAGE using (depending on size) a Tris–Glycin or a Tris–Tricine buffer system and transferred by wet blotting onto a nitrocellulose membrane. The following antibodies were used: BECN1 (Novus, NB500-249 or Cell Signaling, 3495), LC3 (Sigma, L8918), CASP1 and pro-CASP1 (Abcam, ab179515), IL-1beta and pro-IL-1beta (eBioscience, 88701388), NLRP3 (AdipoGen, AG-20B-0014), p62/SQSTM1 (MBL, PM045), CALCOCO2 (Abiocode, R2269-1), and ACTIN (Sigma, A1978). For visualization of the bands, the SuperSignal® West Femto Chemiluminescent Substrate (Thermo, 34096) for detection of horseradish peroxidase activity was used. The quantification of the respective intensities of all bands was achieved with the program ImageJ, and the amount of the respective protein was normalized to the ACTIN protein content.

Phagocytosis assay in acute brain slices

The assay was performed as described before (Krabbe *et al*, 2013). In brief, mice were decapitated and brains were carefully removed and washed in carbogen-saturated artificial cerebrospinal fluid (aCSF), pH 7.4. 130-μm-thick coronal slices were prepared using a vibratome (Microm, Walldorf, Germany) at 4°C and were kept in brain slice buffer at room temperature (21–25°C) for 2 h. The acute brain slices were then incubated with a suspension of FCS-coated yellow-green fluorescent carboxylated microspheres (2 μm diameter, Polysciences Europe GmbH) at a concentration of 1.7×10^7 microspheres/ml for 60 min at 37°C, extensively washed, and finally fixed with 4% paraformaldehyde. Brain sections were stained with anti-Iba1 (Wako, 019-19741) antibody to visualize microglia.

Phagocytosis assay analysis

In brain sections derived from acute brain slices, *z*-stacks of 20 μm thickness were produced using a 40× objective with a step size of 1 μm beginning at the top of the slice, where the microspheres are

 © 2019 The Authors

located. Beads per cell were counted using ImageJ cell counter plugin ensuring that only beads inside a cell were counted as positive. The phagocytic index was determined by assessing the percentage of cells, which contained 0, 1–4, 5–7, 8–10, and > 10 microspheres per cell. The percentage of cells in each group was multiplied by the corresponding grade of phagocytosis (1–4:1, 5–7:2, 8–10:3, > 10:4). The sum of the products in each group was then termed and displayed as phagocytic index (Krabbe *et al*, 2013). Six ROIs (i.e., fields of view) were analyzed per animal.

Histology

Formalin-fixed and sucrose-treated brain hemispheres were frozen and cryosectioned coronally at 30 μm. Tissue sections were collected throughout the entire rostrocaudal extent of the brain and stored at 4°C until staining. Immunohistochemistry and subsequent stereological analyses were performed on 10–12 systematically randomly sampled sections collected at 180-μm intervals for each marker analyzed. Free-floating sections were stained for microglia with the antibody Iba1 (1:500, Wako, 019-19741) or for amyloid-beta using the antibody 4G8 (1:500, Covance, Sig39220-500). Core plaques were stained with Congo red (Carl Roth).

Stereology

Stereology was performed using a Stereo Investigator system (MicroBrightField) and DV-47d camera (MicroBrightField) mounted on a BX53 microscope (Olympus). Stereological quantification of Iba1+ cells and Congo red+ plaques was performed using the optical fractionator method (MicroBrightField). Quantification of 4G8+ plaques was performed using the area fraction fractionator method (MicroBrightField).

Immunocytochemistry

Co-staining of NLRP3 with LC3, p62, mitochondria, or CALCOCO2

Microglia were cultured overnight on Poly-L-Lysine-coated coverslips. For visualization of mitochondria, cells were incubated for 1 h with MitoTracker Red CMX ROS (MTR; Thermo Fisher # M7512) (final concentration 25 nM) prior to stimulation. Autophagosomes were stained according to Ktistakis (Ktistakis, 2015). Shortly, cells were fixed with ice-cold methanol for 10 min and blocked overnight in 1× PBS with 2% bovine serum albumin. LC3 antibody (Sigma, L7543), p62 (Santa Cruz, sc-25575), respectively, and CALCOCO2 antibody (Proteintech, 12229-1-AP) were added for 1 h (1:200), followed by an Alexa568-conjugated secondary antibody (Invitrogen, 11011) for 1 h (1:500). Afterward, the NLRP3 antibody (AdipoGen, AG-20B-0014) was added overnight (1:500), followed by an Alexa488-conjugated secondary antibody (Invitrogen, 11001) for 1 h (1:500).

ASC

Microglia were cultured overnight on Poly-L-Lysine-coated coverslips, fixed with 4% paraformaldehyde for 20 min, permeabilized with 0.1% Triton X-100 for 20 min, blocked with 3% bovine serum albumin for 1–3 h in 1× PBS, and incubated overnight in PBS with the primary antibody ASC (AdipoGen, AG-25B-0006, 1:500). Next day, incubation with an Alexa568-conjugated secondary antibody (Invitrogen, 11011) was performed for 1 h.

Nuclei were counterstained with DAPI (Roche, 10236276001). Samples were mounted with Fluorescent Mounting Medium (Dako, S3023).

Microscopy

Confocal laser scanning microscopy

A Leica TCS SP5 confocal laser scanning microscope controlled by LAS AF scan software (Leica Microsystems, Wetzlar, Germany) was used. Images were taken simultaneously and assembled to stacks. LC3-positive vesicles, NLRP3 aggregates, and ASC specks were counted with the program ImageJ and normalized on the cell area (without the nuclear area), respectively, the cell number. Images in the figures represent maximum image projections.

SIM

3D 3-color SIM images were acquired using the 405, 488, and 568 nm laser lines, standard filter sets, and 125 nm *z*-sectioning of the OMX V4 Blaze (GE Healthcare) system. 100-nm fluorescent beads (TetraSpeck, T7284, Thermo Fisher Scientific) were used for registration of the detection channels, achieving < 40 nm registration error for all three channels. 3D-rendering, image and movie export was done with Arivis Vision4D and ImageJ (Schneider *et al*, 2012).

Image analysis of SIM pictures

The centers (center of mass) of NLRP3 clusters or dapi-stained nuclei were determined in SIM images with Arivis Vision4D using a histogram-based threshold procedure (Otsu's method). NLRP3 clusters were additionally filtered with a size exclusion filter against small objects (minimal diameter 500 nm). 3D radial intensity profiles around cluster centers were generated with a custom-written ImageJ macro (Schneider *et al*, 2012). Averaged intensity values were plotted against their radial distance to the center of mass of single clusters in the reference channel (NLRP3). Distances between NLRP3 clusters and the nucleus were calculated based on the segmentation objects using a custom-written Python script.

Data analysis

Values are presented as mean ± SEM (standard error of the mean). Statistical difference between means was assessed either by the two-tailed *t*-test for two groups or ANOVA with the indicated *post hoc* test for more than two groups using the GraphPad Prism software. Statistically significant values are indicated by $*P < 0.05$, $**P < 0.01$, and $***P < 0.001$.

Expanded View for this article is available online.

Acknowledgements

We are very grateful for the donation of the *Becn1*$^{+/-}$ mice from Tony Wyss-Coray (Stanford University School of Medicine/USA) and intriguing discussions. We thank Anniki Knop and Sebastian Dumkow for excellent technical support. We are indebted to Paul Mohr for support in designing the synopsis image. We would also like to thank Annisa Chand for critical proofreading of the manuscript. This work was supported by the Deutsche Forschungsgemeinschaft (SFB TRR 43, SFB TRR 167, NeuroCure Exc 257, and HE 3130/6-1 to FLH; DFG grant JE278/6-1 to MJ), by the Berlin Institute of Health (BIH; Collaborative Research Grant to FLH), and by the European Union (PHAGO; Innovative

© 2019 The Authors

Medicines Initiative-2). The work of N.G. was supported by the DFG SFB958/Z02 to J.S and the Advanced Medical Bioimaging Core Facility (AMBIO) of the Charite—Universitätsmedizin.

Author contributions

JH, KF, and MJ performed the experimental work and analysis. NG and JS were responsible for the super-resolation microscopy and analysis. MJ and FLH designed the experiments. All authors wrote, revised, and approved the manuscript.

Conflict of interest

The authors declare that they have no conflict of interest.

References

Baroja-Mazo A, Martin-Sanchez F, Gomez AI, Martinez CM, Amores-Iniesta J, Compan V, Barbera-Cremades M, Yague J, Ruiz-Ortiz E, Anton J, Bujan S, Couillin I, Brough D, Arostegui JI, Pelegrin P (2014) The NLRP3 inflammasome is released as a particulate danger signal that amplifies the inflammatory response. *Nat Immunol* 15: 738 – 748

Bracey NA, Gershkovich B, Chun J, Vilaysane A, Meijndert HC, Wright JR Jr, Fedak PW, Beck PL, Muruve DA, Duff HJ (2014) Mitochondrial NLRP3 protein induces reactive oxygen species to promote Smad protein signaling and fibrosis independent from the inflammasome. *J Biol Chem* 289: 19571 – 19584

Butovsky O, Jedrychowski MP, Moore CS, Cialic R, Lanser AJ, Gabriely G, Koeglsperger T, Dake B, Wu PM, Doykan CE, Fanek Z, Liu L, Chen Z, Rothstein JD, Ransohoff RM, Gygi SP, Antel JP, Weiner HL (2014) Identification of a unique TGF-beta-dependent molecular and functional signature in microglia. *Nat Neurosci* 17: 131 – 143

Cho M-H, Cho K, Kang H-J, Jeon E-Y, Kim H-S, Kwon H-J, Kim H-M, Kim D-H, Yoon S-Y (2014) Autophagy in microglia degrades extracellular β-amyloid fibrils and regulates the NLRP3 inflammasome. *Autophagy* 10: 1761 – 1775

Chuang SY, Yang CH, Chou CC, Chiang YP, Chuang TH, Hsu LC (2013) TLR-induced PAI-2 expression suppresses IL-1beta processing via increasing autophagy and NLRP3 degradation. *Proc Natl Acad Sci USA* 110: 16079 – 16084

Faustin B, Lartigue L, Bruey JM, Luciano F, Sergienko E, Bailly-Maitre B, Volkmann N, Hanein D, Rouiller I, Reed JC (2007) Reconstituted NALP1 inflammasome reveals two-step mechanism of caspase-1 activation. *Mol Cell* 25: 713 – 724

Ferreira R, Santos T, Viegas M, Cortes L, Bernardino L, Vieira OV, Malva JO (2011) Neuropeptide Y inhibits interleukin-1beta-induced phagocytosis by microglial cells. *J Neuroinflammation* 8: 169

Fillit H, Ding W, Buee L, Kalman J, Altstiel L, Lawlor B, Wolf-Klein G (1991) Elevated circulating tumor necrosis factor levels in Alzheimer's disease. *Neurosci Lett* 129: 318 – 320

François A, Terro F, Janet T, Bilan A, Paccalin M, Page G (2013) Involvement of interleukin-1β in the autophagic process of microglia: relevance to Alzheimer's disease. *J Neuroinflammation* 10: 1 – 22

Franklin BS, Bossaller L, De Nardo D, Ratter JM, Stutz A, Engels G, Brenker C, Nordhoff M, Mirandola SR, Al-Amoudi A, Mangan MS, Zimmer S, Monks BG, Fricke M, Schmidt RE, Espevik T, Jones B, Jarnicki AG, Hansbro PM, Busto P *et al* (2014) The adaptor ASC has extracellular and "prionoid" activities that propagate inflammation. *Nat Immunol* 15: 727 – 737

Furuya N, Kakuta S, Sumiyoshi K, Ando M, Nonaka R, Suzuki A, Kazuno S, Saiki S, Hattori N (2018) NDP52 interacts with mitochondrial RNA poly(A) polymerase to promote mitophagy. *EMBO Rep* 19: e46363

Ginhoux F, Greter M, Leboeuf M, Nandi S, See P, Gokhan S, Mehler MF, Conway SJ, Ng LG, Stanley ER, Samokhvalov IM, Merad M (2010) Fate mapping analysis reveals that adult microglia derive from primitive macrophages. *Science* 330: 841 – 845

Griffin WS, Stanley LC, Ling C, White L, MacLeod V, Perrot LJ, White CL, Araoz C (1989) Brain interleukin 1 and S-100 immunoreactivity are elevated in Down syndrome and Alzheimer disease. *Proc Natl Acad Sci USA* 86: 7611 – 7615

Harris J, Hartman M, Roche C, Zeng SG, O'Shea A, Sharp FA, Lambe EM, Creagh EM, Golenbock DT, Tschopp J, Kornfeld H, Fitzgerald KA, Lavelle EC (2011) Autophagy controls IL-1β secretion by targeting Pro-IL-1β for degradation. *J Biol Chem* 286: 9587 – 9597

Heneka MT, Kummer MP, Stutz A, Delekate A, Schwartz S, Vieira-Saecker A, Griep A, Axt D, Remus A, Tzeng T-C, Gelpi E, Halle A, Korte M, Latz E, Golenbock DT (2013) NLRP3 is activated in Alzheimer/'s disease and contributes to pathology in APP/PS1 mice. *Nature* 493: 674 – 678

Heppner FL, Ransohoff RM, Becher B (2015) Immune attack: the role of inflammation in Alzheimer disease. *Nat Rev Neurosci* 16: 358 – 372

Holtman IR, Raj DD, Miller JA, Schaafsma W, Yin Z, Brouwer N, Wes PD, Moller T, Orre M, Kamphuis W, Hol EM, Boddeke EW, Eggen BJ (2015) Induction of a common microglia gene expression signature by aging and neurodegenerative conditions: a co-expression meta-analysis. *Acta Neuropathol Commun* 3: 31

Hu Z, Zhou Q, Zhang C, Fan S, Cheng W, Zhao Y, Shao F, Wang HW, Sui SF, Chai J (2015) Structural and biochemical basis for induced self-propagation of NLRC4. *Science* 350: 399 – 404

Inomata M, Niida S, Shibata K, Into T (2012) Regulation of Toll-like receptor signaling by NDP52-mediated selective autophagy is normally inactivated by A20. *Cell Mol Life Sci* 69: 963 – 979

Jo C, Gundemir S, Pritchard S, Jin YN, Rahman I, Johnson GVW (2014) Nrf2 reduces levels of phosphorylated tau protein by inducing autophagy adaptor protein NDP52. *Nat Commun* 5: 3496

Kawarabayashi T, Younkin LH, Saido TC, Shoji M, Ashe KH, Younkin SG (2001) Age-dependent changes in brain, CSF, and plasma amyloid (beta) protein in the Tg2576 transgenic mouse model of Alzheimer's disease. *J Neurosci* 21: 372 – 381

Krabbe G, Halle A, Matyash V, Rinnenthal JL, Eom GD, Bernhardt U, Miller KR, Prokop S, Kettenmann H, Heppner FL (2013) Functional impairment of microglia coincides with beta-amyloid deposition in mice with Alzheimer-like pathology. *PLoS ONE* 8: e60921

Krstic D, Madhusudan A, Doehner J, Vogel P, Notter T, Imhof C, Manalastas A, Hilfiker M, Pfister S, Schwerdel C, Riether C, Meyer U, Knuesel I (2012) Systemic immune challenges trigger and drive Alzheimer-like neuropathology in mice. *J Neuroinflammation* 9: 151 – 151

Ktistakis NT (2015) Monitoring the localization of MAP1LC3B by indirect immunofluorescence. *Cold Spring Harb Protoc* 2015: 751 – 755

Lee HY, Kim J, Quan W, Lee JC, Kim MS, Kim SH, Bae JW, Hur KY, Lee MS (2016) Autophagy deficiency in myeloid cells increases susceptibility to obesity-induced diabetes and experimental colitis. *Autophagy* 12: 1390 – 1403

Lodder J, Denaes T, Chobert MN, Wan J, El-Benna J, Pawlotsky JM, Lotersztajn S, Teixeira-Clerc F (2015) Macrophage autophagy protects against liver fibrosis in mice. *Autophagy* 11: 1280 – 1292

de Luca A, Smeekens SP, Casagrande A, Iannitti R, Conway KL, Gresnigt MS, Begun J, Plantinga TS, Joosten LAB, van der Meer JWM, Chamilos G, Netea MG, Xavier RJ, Dinarello CA, Romani L, van de Veerdonk FL (2014) IL-1 receptor blockade restores autophagy and reduces inflammation in chronic granulomatous disease in mice and in humans. *Proc Natl Acad Sci USA* 111: 3526 – 3531

Lucin KM, O'Brien CE, Bieri G, Czirr E, Mosher KI, Abbey RJ, Mastroeni DF, Rogers J, Spencer B, Masliah E, Wyss-Coray T (2013) Microglial beclin 1 regulates retromer trafficking and phagocytosis and is impaired in Alzheimer's disease. *Neuron* 79: 873 – 886

 © 2019 The Authors

Man SM, Hopkins LJ, Nugent E, Cox S, Gluck IM, Tourlomousis P, Wright JA, Cicuta P, Monie TP, Bryant CE (2014) Inflammasome activation causes dual recruitment of NLRC4 and NLRP3 to the same macromolecular complex. *Proc Natl Acad Sci USA* 111: 7403 – 7408

Menzies FM, Fleming A, Rubinsztein DC (2015) Compromised autophagy and neurodegenerative diseases. *Nat Rev Neurosci* 16: 345 – 357

Menzies FM, Fleming A, Caricasole A, Bento CF, Andrews SP, Ashkenazi A, Fullgrabe J, Jackson A, Jimenez Sanchez M, Karabiyik C, Licitra F, Lopez Ramirez A, Pavel M, Puri C, Renna M, Ricketts T, Schlotawa L, Vicinanza M, Won H, Zhu Y *et al* (2017) Autophagy and neurodegeneration: pathogenic mechanisms and therapeutic opportunities. *Neuron* 93: 1015 – 1034

Mizushima N, Ohsumi Y, Yoshimori T (2002) Autophagosome formation in mammalian cells. *Cell Struct Funct* 27: 421 – 429

Moore AS, Holzbaur EL (2016) Spatiotemporal dynamics of autophagy receptors in selective mitophagy. *Autophagy* 12: 1956 – 1957

Muehlbauer SM, Lima H Jr, Goldman DL, Jacobson LS, Rivera J, Goldberg MF, Palladino MA, Casadevall A, Brojatsch J (2010) Proteasome inhibitors prevent caspase-1-mediated disease in rodents challenged with anthrax lethal toxin. *Am J Pathol* 177: 735 – 743

von Muhlinen N, Akutsu M, Ravenhill BJ, Foeglein Á, Bloor S, Rutherford TJ, Freund SM, Komander D, Randow F (2013) An essential role for the ATG8 ortholog LC3C in antibacterial autophagy. *Autophagy* 9: 784 – 786

Murthy A, Li Y, Peng I, Reichelt M, Katakam AK, Noubade R, Roose-Girma M, DeVoss J, Diehl L, Graham RR, van Lookeren Campagne M (2014) A Crohn/'s disease variant in Atg16l1 enhances its degradation by caspase 3. *Nature* 506: 456 – 462

Patel NS, Paris D, Mathura V, Quadros AN, Crawford FC, Mullan MJ (2005) Inflammatory cytokine levels correlate with amyloid load in transgenic mouse models of Alzheimer's disease. *J Neuroinflammation* 2: 9 – 9

Perry VH, Holmes C (2014) Microglial priming in neurodegenerative disease. *Nat Rev Neurol* 10: 217 – 224

Pickford F, Masliah E, Britschgi M, Lucin K, Narasimhan R, Jaeger PA, Small S, Spencer B, Rockenstein E, Levine B, Wyss-Coray T (2008) The autophagy-related protein beclin 1 shows reduced expression in early Alzheimer disease and regulates amyloid β accumulation in mice. *J Clin Invest* 118: 2190 – 2199

Prokop S, Miller KR, Heppner FL (2013) Microglia actions in Alzheimer's disease. *Acta Neuropathol* 126: 461 – 477

Qu X, Yu J, Bhagat G, Furuya N, Hibshoosh H, Troxel A, Rosen J, Eskelinen EL, Mizushima N, Ohsumi Y, Cattoretti G, Levine B (2003) Promotion of tumorigenesis by heterozygous disruption of the beclin 1 autophagy gene. *J Clin Invest* 112: 1809 – 1820

Radde R, Bolmont T, Kaeser SA, Coomaraswamy J, Lindau D, Stoltze L, Calhoun ME, Jaggi F, Wolburg H, Gengler S, Haass C, Ghetti B, Czech C, Holscher C, Mathews PM, Jucker M (2006) Abeta42-driven cerebral amyloidosis in transgenic mice reveals early and robust pathology. *EMBO Rep* 7: 940 – 946

Saitoh T, Fujita N, Jang MH, Uematsu S, Yang BG, Satoh T, Omori H, Noda T, Yamamoto N, Komatsu M, Tanaka K, Kawai T, Tsujimura T, Takeuchi O, Yoshimori T, Akira S (2008) Loss of the autophagy protein Atg16L1 enhances endotoxin-induced IL-1beta production. *Nature* 456: 264 – 268

Santeford A, Wiley LA, Park S, Bamba S, Nakamura R, Gdoura A, Ferguson TA, Rao PK, Guan JL, Saitoh T, Akira S, Xavier R, Virgin HWT, Apte RS (2016) Impaired autophagy in macrophages promotes inflammatory eye disease. *Autophagy* 12: 1876 – 1885

Schneider CA, Rasband WS, Eliceiri KW (2012) NIH Image to ImageJ: 25 years of image analysis. *Nat Methods* 9: 671 – 675

Shi CS, Shenderov K, Huang NN, Kabat J, Abu-Asab M, Fitzgerald KA, Sher A, Kehrl JH (2012) Activation of autophagy by inflammatory signals limits IL-1beta production by targeting ubiquitinated inflammasomes for destruction. *Nat Immunol* 13: 255 – 263

Squires RC, Muehlbauer SM, Brojatsch J (2007) Proteasomes control caspase-1 activation in anthrax lethal toxin-mediated cell killing. *J Biol Chem* 282: 34260 – 34267

Subramanian N, Natarajan K, Clatworthy MR, Wang Z, Germain RN (2013) The adaptor MAVS promotes NLRP3 mitochondrial localization and inflammasome activation. *Cell* 153: 348 – 361

Susjan P, Roskar S, Hafner-Bratkovic I (2017) The mechanism of NLRP3 inflammasome initiation: trimerization but not dimerization of the NLRP3 pyrin domain induces robust activation of IL-1beta. *Biochem Biophys Res Comm* 483: 823 – 828

Swinnen N, Smolders S, Avila A, Notelaers K, Paesen R, Ameloot M, Brone B, Legendre P, Rigo JM (2013) Complex invasion pattern of the cerebral cortex bymicroglial cells during development of the mouse embryo. *Glia* 61: 150 – 163

Tay TL, Savage JC, Hui CW, Bisht K, Tremblay ME (2017) Microglia across the lifespan: from origin to function in brain development, plasticity and cognition. *J Physiol* 595: 1929 – 1945

Tumbarello DA, Manna PT, Allen M, Bycroft M, Arden SD, Kendrick-Jones J, Buss F (2015) The autophagy receptor TAX1BP1 and the molecular motor myosin VI are required for clearance of salmonella typhimurium by autophagy. *PLoS Pathog* 11: e1005174

Ulland TK, Song WM, Huang SC, Ulrich JD, Sergushichev A, Beatty WL, Loboda AA, Zhou Y, Cairns NJ, Kambal A, Loginicheva E, Gilfillan S, Cella M, Virgin HW, Unanue ER, Wang Y, Artyomov MN, Holtzman DM, Colonna M (2017) TREM2 maintains microglial metabolic fitness in Alzheimer's disease. *Cell* 170: 649 – 663.e613

Van Opdenbosch N, Gurung P, Vande Walle L, Fossoul A, Kanneganti TD, Lamkanfi M (2014) Activation of the NLRP1b inflammasome independently of ASC-mediated caspase-1 autoproteolysis and speck formation. *Nat Commun* 5: 3209

Verlhac P, Viret C, Faure M (2015) Dual function of CALCOCO2/NDP52 during xenophagy. *Autophagy* 11: 965 – 966

Vom Berg J, Prokop S, Miller KR, Obst J, Kalin RE, Lopategui-Cabezas I, Wegner A, Mair F, Schipke CG, Peters O, Winter Y, Becher B, Heppner FL (2012) Inhibition of IL-12/IL-23 signaling reduces Alzheimer's disease-like pathology and cognitive decline. *Nat Med* 18: 1812 – 1819

Walsh JG, Muruve DA, Power C (2014) Inflammasomes in the CNS. *Nat Rev Neurosci* 15: 84 – 97

Wang D, Zhang J, Jiang W, Cao Z, Zhao F, Cai T, Aschner M, Luo W (2017) The role of NLRP3-CASP1 in inflammasome-mediated neuroinflammation and autophagy dysfunction in manganese-induced, hippocampal-dependent impairment of learning and memory ability. *Autophagy* 13: 914 – 927

Ye J, Jiang Z, Chen X, Liu M, Li J, Liu N (2017) The role of autophagy in pro-inflammatory responses of microglia activation via mitochondrial reactive oxygen species *in vitro*. *J Neurochem* 142: 215 – 230

Yue Z, Jin S, Yang C, Levine AJ, Heintz N (2003) Beclin 1, an autophagy gene essential for early embryonic development, is a haploinsufficient tumor suppressor. *Proc Natl Acad Sci USA* 100: 15077 – 15082

Zhang L, Chen S, Ruan J, Wu J, Tong AB, Yin Q, Li Y, David L, Lu A, Wang WL, Marks C, Ouyang Q, Zhang X, Mao Y, Wu H (2015) Cryo-EM structure of the activated NAIP2-NLRC4 inflammasome reveals nucleated polymerization. *Science* 350: 404 – 409

Zhang D, Wang W, Sun X, Xu D, Wang C, Zhang Q, Wang H, Luo W, Chen Y, Chen H, Liu Z (2016) AMPK regulates autophagy by phosphorylating BECN1 at threonine 388. *Autophagy* 12: 1447 – 1459

Zhou R, Yazdi AS, Menu P, Tschopp J (2011) A role for mitochondria in NLRP3 inflammasome activation. *Nature* 469: 221 – 225

© 2019 The Authors

Mein Lebenslauf wird aus datenschutzrechtlichen Gründen in der elektronischen Version meiner Arbeit nicht veröffentlicht

Mein Lebenslauf wird aus datenschutzrechtlichen Gründen in der elektronischen Version meiner Arbeit nicht veröffentlicht

Publication List

Beclin1-driven autophagy modulates the inflammatory response of microglia via NLRP3
Judith Houtman, Kiara Freitag, Niclas Gimber, Jan Schmoranzer, Frank L. Heppner, Marina Jendrach. *The EMBO Journal (2019) e9943*

The Amyloid-beta rich CNS environment alters myeloid cell functionality independent of their origin
Natalia Drost§, Judith Houtman§, Zoltán Cseresnyés, Raluca Niesner, Jan-Leo Rinnenthal, Kelly R Miller, Stefan Prokop&, Frank L Heppner&
In revision

Acknowledgments

Frank, thank you for giving me a chance to do a neuroscience PhD as a non-neuroscientist, and for supporting me throughout these years. Thank you for always appreciating my work, even when it was the umpteenth 'neutral' result I showed you, and for teaching me how rewarding persistence is.

Marina, I could not have written this publication based thesis without you. Thank you, for being a beacon of knowledge on autophagy, cell culture and all that's lab related, for accompanying me to conferences, for sharing frustration and excitement, and for always having my best interest at heart.

To everyone I worked with in the AZH, thank you for welcoming me into the lab, for teaching me so many things I don't even know where to start, for technical and philosophical discussions, for helping me become a neuroscientist, and for letting me share my knowledge with you in return.

Alex I, Alex II, Corinna, Eileen, Jan, Kiara, Pascale, Shirin, thank you for making work feel like a pleasant pastime, for sharing frustrations, for organizing the lab together, for 'Motivationstanz', hugs and Sekt whenever appropriate, pizza and movie nights, and many more things. Thank you for being the very best colleagues one can wish for!

Magdalena, thanks for sharing our experiences during these 5 years, for discussing our experiments, frustrations, future perspectives, and less serious matters.

Mariska, Joy, Linda, Chantal, Merel, Eline, Joost, ik ben blij dat onze vriendschap niet te erg lijdt onder het feit dat ik ‚zooo-ver-weg' ben. Bedankt voor jullie support en regelmatige weekend bezoekjes aan Berlijn.

Toon, Diny, Marieke, Nick, bedankt voor jullie interesse en support, en voor de gezellige weekenden in Duitsland en Nederland.

Pap en Mam, Ramon, Claudia, Femke, Jan Willem, bedankt voor jullie steun over de afgelopen 5 jaar en de continue interesse in mijn muizen. Van jullie bezoekjes aan Berlijn krijg ik soms een beetje heimwee, maar met regelmatige skype dates zijn jullie eigenlijk super dichtbij.

Wouter, lief, bedankt voor je interesse in mijn favoriete onderzoeksveld, voor de wetenschappelijke discussies, voor je eindeloze begrip en geduld, voor het inzicht dat genieten van je vrije tijd betere werkresultaten oplevert, en dat je zorgt dat ik dat inzicht ook in de praktijk breng.